Measurement 199 (2022) 111591

Contents lists available at ScienceDirect

Measurement

journal homepage: www.elsevier.com/locate/measurement

Output-only structural damage identification using hybrid Jaya and differential evolution algorithm with reference-free correlation functions

Guangcai Zhang [a], Chunfeng Wan [a,*], Xiaobing Xiong [a], Liyu Xie [b], Mohammad Noori [c], Songtao Xue [b,d,*]

[a] Key Laboratory of Concrete and Prestressed Concrete Structure of Ministry of Education, Southeast University, Nanjing, China
[b] Research Institute of Structural Engineering and Disaster Reduction, College of Civil Engineering, Tongji University, Shanghai, China
[c] Department of Mechanical Engineering, California Polytechnic State University, San Luis Obispo, USA
[d] Department of Architecture, Tohoku Institute of Technology, Sendai, Japan

ARTICLE INFO

Keywords:
Structural damage identification
Jaya algorithm
Differential evolution algorithm
Hybrid algorithm
Adjacent acceleration correlation function
Gradient search method

ABSTRACT

To solve the optimization-based structural damage identification problem, a novel hybrid algorithm based on Jaya and differential evolution algorithm (HJDEA) is proposed to detect, locate and quantify structural damages by effectively incorporating the powerful local exploitation capacity of Jaya algorithm and global exploration capability of differential evolution. Meanwhile, Hammersley sequence initialization and Lévy flight search mechanism are introduced into HJDEA to further improve convergence rate and refining the quality of the best solution. Four different algorithms, genetic algorithm, particle swarm optimization, Jaya and the proposed HJDEA are employed for comparative study. In addition, the objective function is established by adjacent acceleration correlation function so as to avoid false identification caused by defining improper reference point. The performance of the proposed damage identification strategy based on HJDEA and adjacent acceleration correlation function is investigated with numerical examples involving an 8-DOF lumped mass model and a cantilever beam, as well as an experimental study of the ASCE benchmark structure under white noise excitation. Results show that the proposed hybrid identification method is accurate, efficient and robust in the identification of the damage existence, location and severity of stiffness and mass parameters even with partial output-only responses and 20% noise-polluted measurements.

1. Introduction

Major civil engineering structures, such as super high-rise buildings, large-span spatial structures and bridges, nuclear power plants, offshore production platforms, and underground comprehensive pipe galleries, have a design service life of over decades or even one hundred years. During the long-term service period, structures would inevitably accumulate damages due to earthquakes, typhoons, as well as the coupling effect of adverse factors such as environmental erosion, material degradation, corrosion and overload. If the damaged members are not detected and repaired in time, such potential threat may lead to the collapse of the whole structure, causing catastrophic accidents. Therefore, it is of great theoretical and practical significance to conduct structural health monitoring and damage identification to ensure the structural safety, meanwhile reduce the operation and maintenance costs.

After decades of development, considerable number of damage identification methods have been proposed, among which the vibration-based damage identification methods are able to inversely identify structural changes for the physical properties of stiffness, mass, damping, etc., with its dynamic responses (displacement, velocity, acceleration, strain) collected from sensors embedded in the structure, and fruitful research results are achieved [1]. They can be broadly divided into two categories for the vibration-based damage identification methods, namely frequency domain and time domain methods. Some frequency domain methods have been widely applied for structural damage assessment especially for the case of unknown input information. However, modal indexes, such as natural frequencies [2], mode shapes [3], modal strain energy [4], mode shape curvature [5], may have their inherent disadvantages. In fact, natural frequencies as a

* Corresponding authors at: Key Laboratory of Concrete and Prestressed Concrete Structure of Ministry of Education, Southeast University, Nanjing, China (C. Wan); Research Institute of Structural Engineering and Disaster Reduction, College of Civil Engineering, Tongji University, Shanghai, China (S. Xue).
E-mail addresses: wan@seu.edu.cn (C. Wan), xue@tongji.edu.cn (S. Xue).

https://doi.org/10.1016/j.measurement.2022.111591
Received 27 April 2022; Received in revised form 13 June 2022; Accepted 1 July 2022
Available online 5 July 2022

global index of structural vibration characteristics are insensitive to the local or minor damages of structural members. Compared with the natural frequencies, high-order mode shapes are much sensitive to local damages. However, high-order modes are difficult to be accurately acquired and susceptible to be polluted by measurement noise. Besides, it might be challenging to identify structural damage with these model data when affected by environment variation. In contrast, numerous time domain methods have been developed to detect structural damage directly using raw measurement responses. Although the least square method [6], the extended Kalman filter [7], the particle filter [8], the response sensitivity method [9] and wavelet analysis [10] etc. have proven their capacity to identify structural damage, most of aforementioned traditional methods generally require a good initial point or appropriate gradient information, which adversely affects their practical application in large-scale and complex structures.

For most of structural identification methods in time domain, the information of input excitation and output responses are generally required simultaneously. However, the time history of excitations applied to engineering structures, such as wind load, traffic load, are difficult to be directly measured, whereas some efforts have been made to successfully identify the damages only with the structural output responses without excitation measurement. A structural damage identification method based on the cross correlation function amplitude vector was proposed [11], and the experimental results of a composite beam model verified its ability to locate damages under steady random excitation. A modified covariance of covariance matrix-based damage identification method was developed [12], and the numerical results of a simply supported beam indicated that this method was insensitive to noise. In addition, an auto/cross-correlation function of acceleration-based method was presented to identify the structural damage under multiple random excitations [13]. On this basis, correlation functions and four evolutionary algorithms were combined to identify structural parameters [14]. However, reference point is necessarily defined and plays an important role in these researches. If the response at the reference point has poor sensitivity to the structural damage, identification accuracy of cross-correlation function may be adversely affected [15]. To address this deficiency, a new method based on adjacent acceleration correlation function is introduced, which do not need to predefine reference point. Accordingly, the proposed method can avoid obtaining wrong damage identification results caused by selecting inappropriate reference points.

In recent years, with the advancement of available computational capacity, non-traditional identification methods, e.g., neural network methods and heuristic optimization algorithms, have received increasing attention and become attractive alternative strategies. Neural networks have the features of parallel computing, self-learning, nonlinear mapping and robustness, presenting pleasant computational results in the damage identification of hyperbolic cooling towers [16] and bolt-loosening [17], while significant number of training samples and demanding computational resources are needed. Compared with traditional methods, some of the well-known heuristic optimization algorithms such as genetic algorithm (GA) [18], particle swarm optimization (PSO) [19] algorithm, differential evolution (DE) algorithm [20], evolutionary strategy [21], have more powerful performance to deal with multi-objective, nonlinear, discontinuous or discrete complex optimization problems. Accordingly, heuristic algorithms have attracted increasing attention in the field of structural damage identification due to their advantages of strong search ability, ease of implementation and loose initial conditions. However, it should be noted that structural damage identification is a typical inverse problem with limited output but considerable unknowns to be identified, which may pose some challenges to above-mentioned heuristic algorithms, especially taking the environmental noise, incomplete measurements, modelling error, etc. into account. Therefore, more population-based metaheuristic algorithms, such as ant colony optimization [22], frog-leaping algorithm [23], artificial bee colony algorithm [24], butterfly optimization algorithm [25], grey wolf optimization algorithm [26], whale Optimization Algorithm [27], are increasingly developed and employed. These novel algorithms have succeeded in solving various optimization problems, such as training wavelet neural networks [28], structural parameters identification [29] and cloud computing resource scheduling [30], but considerable computational time still have to be consumed. More importantly, for the aforementioned swarm intelligence optimization algorithms, the algorithm-specific parameters are generally required, which would dramatically affect its effectiveness to solve optimization problems [31]. Possibly, changing a single algorithm parameter may result in evident alteration of the computational results. In other words, unsatisfied identification results or local optimal solution will be obtained if algorithm parameters are set inappropriately. Therefore, repeated trial-and-error procedures are usually required to find suitable coefficients before solving different optimization problems, which would inevitably waste considerable computational resources.

An emerging yet powerful swarm intelligence optimization algorithm without any algorithm-specific parameters except two common parameters, i.e., population size and number of maximum iterations, was proposed by Rao and named Jaya algorithm [32]. The core idea of Jaya algorithm is that offspring moves toward the optimal solution and meanwhile away from the inferior solution, resulting in progressive improvement for the quality of solutions. Diverse real-world optimization applications have been achieved by Jaya algorithm, e.g., parameters identification of photovoltaic cell and module models [33], optimization of shell-and-tube heat exchangers [34], design of dual-input power system stabilizer [35], job-shop scheduling problem optimization [36] and text document clustering [37]. Despite the fact that Jaya algorithm has demonstrated better performance than genetic algorithm, particle swarm optimization, teaching optimization algorithm and artificial bee colony algorithm in standard function test and some engineering optimization design, it still suffers by the problems of slow convergence speed and easy to be trapped into local optimal solution [38]. The simple mutation mechanism of basic Jaya algorithm may pose challenges of application in solving the optimization-based structural damage identification problem, especially for the large-scale and complex structural systems where considerable number of unknown parameters and degrees of freedom involved. In recent years, there have been some studies to improve the performance of Jaya algorithm Yu et al. [39] proposed a performance-guided Jaya algorithm by introducing individual performance quantification and self-adaptive chaotic perturbation mechanisms. Farah et al. [40] embedded chaotic sequences into Jaya algorithm to alleviate the drawbacks of premature convergence, demonstrating more robust performance on the test functions than other algorithms. Warid et al. [41] developed a novel quasi-oppositional modified Jaya algorithm as a promising method to solve different multi-objective optimal power flow problems.

In addition to further exploring new improvement mechanisms to enhance the optimization capacity of Jaya algorithm, hybrid algorithm by integrating different swarm intelligence algorithms provides another attractive way with a large number of successful applications, such as hybrid particle swarm optimization with improved Nelder–Mead algorithm [42], hybrid butterfly optimization and differential evolution algorithm [43], hybrid charged system search and colliding bodies optimization algorithm [44], hybrid difference grey wolf algorithm [45]. In this study, a hybrid algorithm based on Jaya algorithm and differential evolution algorithm (HJDEA) is proposed by effectively incorporating the merits of the exploitation capability of Jaya algorithm and exploration capability of differential evolution algorithm. Besides, population initialization with Hammersley sequence is employed to increases the diversity of the population and the convergence speed of hybrid algorithm. Lévy flight search mechanism is implemented to refine the quality of the optimal solution and escape from the local optimum. Thus, for, the balance between exploiting the previous region and exploring new search domain might be better achieved than original Jaya algorithm. The proposed HJDEA has powerful global exploration

capacity, fast convergence speed in the early stage, while it might manifest unacceptable slow computational efficiency due to its stochastic characteristic of parameter searching, especially when the identified solution approaches to the neighborhood of the global optimum.

The local damages of structures are considered as reduction of elemental stiffness parameters, and the alteration of mass parameters is directly ignored in the previous studies [42,43]. However, structural local damages may be accompanied by the simultaneous reduction of mass and stiffness parameters owing to the local spalling of concrete or elements removed from structure etc. In addition, in some circumstances, it is quite difficult to visually inspect whether the mass parameters are changed [46]. Thus, to more accurately express the structural damage model, it is suggested that both the variation of stiffness parameters and mass parameters be considered.

In this paper, a novel damage identification strategy based on proposed HJDEA and adjacent acceleration correlation function is proposed to simultaneously identify the alterations of both stiffness and mass parameters with output-only responses under white noise excitation. In the proposed hybrid algorithm, the powerful local search capability of Jaya and global search capability of DE are effectively combined. Meanwhile, other improvements including Hammersley sequence initialization and Lévy flight search mechanism are also introduced. Adjacent acceleration correlation function is developed to establish the objective function. First, the performance of the proposed HJDEA is evaluated and compared with GA, PSO and Jaya algorithms by numerical studies on an 8-DOF lumped mass model. Then, the effectiveness of proposed reference point-free method on accuracy and efficiency of damage identification is validated with a cantilever beam structure. In addition, the ASCE Benchmark structure are employed to test the applicability of the proposed output-only method based on HJDEA and adjacent acceleration correlation function to structural damage identification. Finally, to further accelerate convergence rate and improve identification accuracy, a hybrid approach based on the proposed HJDEA and gradient search method is proposed and investigated with the attractive idea of converging to the region of optimal solution by HJDEA and then taking it as initial values in the subsequent gradient search.

2. Identification algorithms

In this section, basic Jaya algorithm and differential evolution are briefly introduced, respectively. Then, the hybrid Jaya and differential evolution algorithm is proposed and described in detail.

2.1. Jaya algorithm

Jaya algorithm is a recently proposed global search-based swarm intelligence optimization algorithm to solve constrained and unconstrained optimization problems. A distinctive feature of Jaya algorithm is that algorithm-specific parameters, such as mutation operator, crossover operator, inertia weight, learning factors, are not required. The structure of Jaya algorithm is presented in Fig. 1, which can be roughly divided into four steps: initialization, individual updating, greedy selection, and result output.

Jaya algorithm randomly initializes population in the predefined search space as follows.

$$X_{i,j} = L_{i,j} + rand(0,1) \times \left(U_{i,j} - L_{i,j}\right) \tag{1}$$

where $U_{i,j}$ and $L_{i,j}$ stand for the upper and lower bound of the search limits, respectively; $rand(0,1)$ is a random number taken from the range of [0, 1].

After the step of initialization, fitness function evaluations are implemented and ranked for all candidate solutions in the current colony. Subsequently, the best individual X_{best} and the worst one X_{worst} can be easily determined. Then, individuals are updated to generate offspring $X'_{i,j,G}$ with the best and the worst candidates by following equation.

$$X'_{i,j,G} = X_{i,j,G} + rand_1 \times \left(X_{best,j,G} - \left|X_{i,j,G}\right|\right) - rand_2 \times \left(X_{worst,j,G} - \left|X_{i,j,G}\right|\right) \tag{2}$$

where $X_{i,j,G}$ and $\left|X_{i,j,G}\right|$ denote the j-th variable of the i-th candidate solution at the G-th iteration and its absolute value, respectively; $rand_1$ and $rand_2$ stand for random numbers taken from the interval [0, 1]; $X_{best,j,G}$ and $X_{worst,j,G}$ represent the value of the j-th variable for the best and worst candidate solutions in iteration of G, respectively; On the right side of Eq. (2), the second term $rand_1 \times \left(X_{best,j,G} - \left|X_{i,j,G}\right|\right)$ implies the tendency of candidates to approach the optimal solution while the third term $rand_2 \times \left(X_{worst,j,G} - \left|X_{i,j,G}\right|\right)$ indicates the trend of candidates to move away from the worst solution.

The third step is greedy selection, which can make the solution with better fitness function value survive to next generation by comparing the new solution with the previous one.

$$X_{i,G+1} = \begin{cases} X'_{i,G} & f(X'_{i,G}) \leqslant f(X_{i,G}) \\ X_{i,G} & otherwise \end{cases} \tag{3}$$

Step 1. Initialization
  Predefine the population size *NP*, the dimension of variables *Dim*, maximum generation G_m
  Randomly produce initial population with Eq. (1)
  Define fitness function
Step 2. Individual updating
  While maximum generation G_m is not reached **do**
    Compute fitness values and find the best individual X_{best} and the worst individual X_{worst}
    For candidate i = 1 to *NP* **do**
      For variable j=1 to *Dim* **do**
        Produce random number in the interval of [0, 1]
        Update individual $X_{i,j}$ with Eq. (2)
      End for
      Evaluate the fitness value of the updated individual
    End for
Step 3. Greedy selection
    Implement greedy selection strategy to keep better solution
    Update current number of iterations
  End while
Step 4. Result output
  Output the best solution and optimal value

Fig. 1. The structure of Jaya algorithm.

where $X_{i,G+1}$ and $X_{i,G}$ mean the i-th individual at G-th and $(G+1)$-th iteration, respectively; $X'_{i,G}$ is the updated value of$X_{i,G}$; f denotes fitness function evaluation.

The second and third steps will be performed until the convergence criterion satisfied or the predefined maximum iteration number reached. Finally, output the identified optimal solution.

2.2. Differential evolution algorithm

As a typical representative of stochastic search algorithms, differential evolution algorithm has powerful global optimization capacity. After initializing the population, mutation operation is implemented through differential strategy of parent individuals. A popular variant of mutation formulas is presented as.

$$V_{i,G+1} = X_{r1,G} + F \times \left(X_{r2,G} - X_{r3,G} + X_{r4,G} - X_{r5,G}\right) \tag{4}$$

where $V_{i,G+1}$ means the mutation vector; $X_{r1,G}, X_{r2,G}, X_{r3,G}, X_{r4,G}, X_{r5,G}$ denote five different candidates randomly selected from the population; F stands for the mutation factor taken from the range of [0, 2].

Then, the crossover operation is conducted by crossing the parent vector with the corresponding mutation vector. The new offspring individual can be generated by.

$$T_{i,j,G+1} = \begin{cases} V_{i,j,G+1} & if(rand(j) \leqslant CR) or(j = randn(i)) \\ X_{i,j,G} & otherwise \end{cases} \tag{5}$$

where$i = 1, 2, ..., NP, j = 1, 2, ..., N$, NP and N represent the number of individuals and variables, respectively; CR is the crossover factor within the range of [0, 1].

Finally, the greedy selection strategy is utilized in every iteration to guide the algorithm approximate the optimal solution by retaining superior individuals and eliminating inferior individuals.

2.3. Hybrid Jaya and differential evolution algorithm

2.3.1. Initialization with Hammersley sequence

In general, the initial population of swarm intelligence algorithms are randomly generated within given search space. Nevertheless, potential instability may render the optimization algorithm trapped into local optimum when the initial individuals coincidentally distribute a limited local region, which is extremely unfavorable to the subsequent stochastic search. To this end, some modified initialization methods have been introduced, such as Logistic mapping [47], Tent mapping [48] and low-discrepancy sequences [49], to generate more uniform samples than random sequence. Logistic mapping and Tent mapping are representative methods to produce chaotic sequences, widely applied in various algorithm improvements due to its characteristics of randomness and ergodicity. Besides, it was found that quasi-Monte Carlo methods or low-discrepancy sequences provide another favorable alternative, especially for Hammersley sequence owing to its inherent advantage of highly uniform distribution [49]. A brief description of Hammersley sequence is given in the following content.

Hammersley sequence uses the characteristic of computer's binary representation to mirror the binary representation of a given decimal number after the decimal point, and constructs a value between [0,1] through the radical inversion method.

$$n = \sum_{b=0}^{z} n_b P^b = n_z P^z + ... + n_1 P^1 + n_0 P^0 \tag{6}$$

where n means any integer; $z = \left\lfloor \log_p(n) \right\rfloor$; stands for extracting the integer part of the internal number.

Then, the value of n can be expressed as.

$$\varphi_P(n) = n_0 P^{-1} + n_1 P^{-2} + ... + n_z P^{-z-1} = \sum_{m=0}^{z} n_m P^{-m-1} \tag{7}$$

where $\varphi_P(n)$ denotes the value of n after the step of radical inversion.

Hammersley sequence in k-dimensional space could be easily generated by.

$$\psi_k(n) = (n/N, \varphi_P(n)) = \left(n/N, \varphi_{P_1}(n), \varphi_{P_2}(n), ..., \varphi_{P_{k-1}}(n)\right) \tag{8}$$

where$n = 0, 1, ..., N-1$; N represents the total number of sampling points; $P_1, P_2, ..., P_{k-1}$ are prime numbers.

Four initialization methods, namely Logistic mapping, Tent mapping, random sequence and Hammersley sequence, are reasonably compared. One-dimensional distributions of 100 samples for four different initialization methods are presented in Fig. 2 and Table 1. It is obviously observed that Hammersley sequence is capable of constructing the most uniform set of samples among the four methods, which would facilitate generating uniform initial population within the whole search space, increasing population diversity and improving convergence efficiency. Therefore, only Hammersley sequence is applied in hybrid algorithm as follows.

$$X_{i,j} = L_{i,j} + \psi(i,j) \times \left(U_{i,j} - L_{i,j}\right) \tag{9}$$

where $\psi(i,j)$ represents samples generated by Hammersley sequence.

2.3.2. Lévy flight search mechanism

Lévy flight is a kind of random walk whose step sizes follow Lévy distribution, and it can make large "jumps'' to a new region of the search domain. From Eq. (2), it is clear that the best solution of Jaya algorithm plays an important role in the search process by guiding and drawing other individuals to move to its location. However, the identified best individual may be located in the local optimal region when solving complex multi-peak optimization problems. Accordingly, other individuals within the population would be easily attracted to the position of the current local best solution, leading to premature convergence due to trapped into local optima. Lévy flight search mechanism has been adopted in many swarm intelligence algorithms, such as, cuckoo search algorithm, fruit fly optimization algorithm, tree seeds algorithm, bat algorithm, to help the best solution escape from the local optimum.

New individual of next generation X_{i+1} can be generated by Lévy flight as follows.

$$X_{i+1} = X_i + \kappa \oplus D(\lambda) \tag{10}$$

where κ is the step size parameter; $\oplus$ means entry wise multiplication; λ stands for distribution index,$0 < \lambda \leqslant 2$.

The step size based on Lévy flight can be expressed as.

$$step = \kappa \oplus D(\lambda) \sim 0.1 \frac{u}{|v|^{1/\lambda}} (X_r - X_{best}) \tag{11}$$

where X_{best} is the best solution in the current iteration; X_r represents a randomly selected individual,$X_r \neq X_{best}$; u and v obey following normal distribution.

$$u \sim N\left(0, \sigma_u^2\right), v \sim N\left(0, \sigma_v^2\right) \tag{12}$$

$$\sigma_u = \left\{ \frac{\Gamma(1+\lambda) \times \sin(\pi\lambda/2)}{\Gamma\left[(1+\lambda)/2\right] \times \lambda \times 2^{(\lambda-1)/2}} \right\}^{1/\lambda}, \sigma_v = 1 \tag{13}$$

where Γ denotes Gamma function.

A new updating equation of best solution X_{best} is introduced as.

$$X^*_{best} = X_{best} + step \times rand(0,1) \tag{14}$$

where X^*_{best} is the best solution after performing Lévy flight; $step \times rand(0,1)$ means the process of Lévy flight.

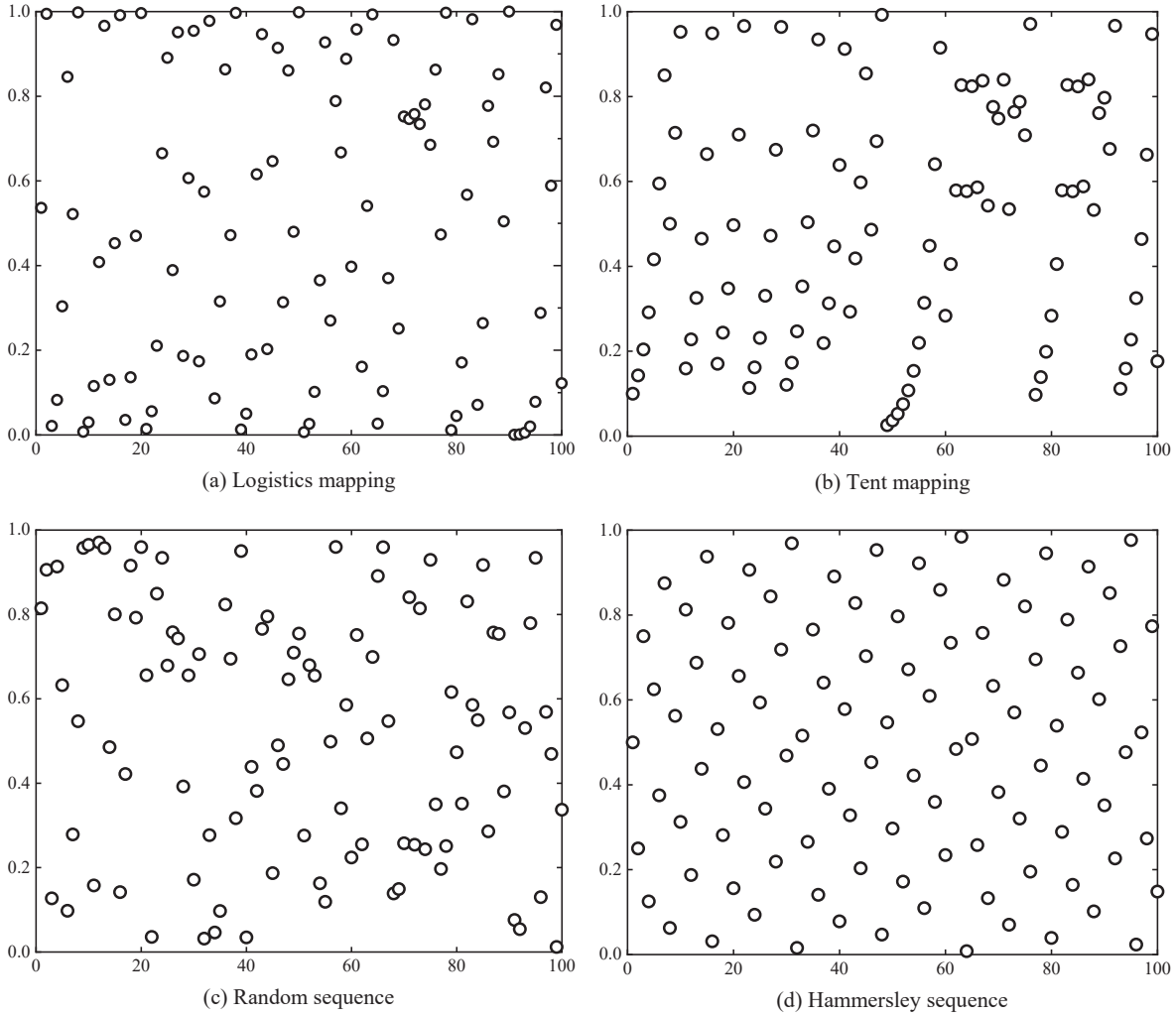

Fig. 2. One-dimensional distribution of 100 samples with four initialization methods.

Table 1
Statistical results of four different initialization methods.

Domain	Number of samples			
	Logistic mapping	Tent mapping	Random sequence	Hammersley sequence
0.0–0.2	32	20	19	20
0.2–0.4	13	19	18	20
0.4–0.6	13	24	17	20
0.6–0.8	14	17	23	20
0.8–1.0	28	20	23	20

Finally, the solution with better fitness value between X_{best} and X^*_{best} will survive to the next generation.

2.3.3. Mutation learning mechanism

It can be seen from Eq. (2) that individuals of Jaya algorithm are updated considering both the best and worst candidates, which is conducive to accelerating the convergence speed and improving the local optimization ability, yet the diversity of the population and global optimization ability of Jaya algorithm may decrease with the increasement of iteration numbers, resulting in the imbalance between exploration and exploitation. To alleviate this issue, a novel mutation learning mechanism inspired by the Eq. (4) is introduced into Jaya algorithm as follows.

$$V_{i,G+1} = X_{r1,G} + rand_1 \times \left(X_{r2,G} - X_{r3,G}\right) + rand_2 \times \left(X_{r4,G} - X_{r5,G}\right) \tag{15}$$

where $X_{r1,G}, X_{r2,G}, X_{r3,G}, X_{r4,G}$ and $X_{r5,G}$ stand for five different candidates randomly selected from the population at G-th generation,; and are random numbers within the range of [0, 1].

The new solution $V_{i,G+1}$ is obtained from the mutation operation of five different individuals. Thus, the proposed mutation learning mechanism can sufficiently utilize existed information of other individuals and improve global search capacity.

2.3.4. Framework of hybrid algorithm

The hybrid Jaya and differential evolution algorithm is proposed by introducing population initialization with Hammersley sequence, Lévy flight search mechanism and mutation learning mechanism into basic Jaya algorithm. It should be noted that this HJDEA effectively combines the merits of each single algorithm, namely, the powerful exploitation capability of Jaya algorithm and exploration capability of differential evolution algorithm. Besides, there are no additional algorithm parameters introduced, which means HJDEA does not require any algorithm parameters except for two general parameters, i.e., population size and number of iterations. Hence, the proposed hybrid algorithm has the advantages of simple structure, high stability and easiness of operation. Its flowchart is presented in Fig. 3.

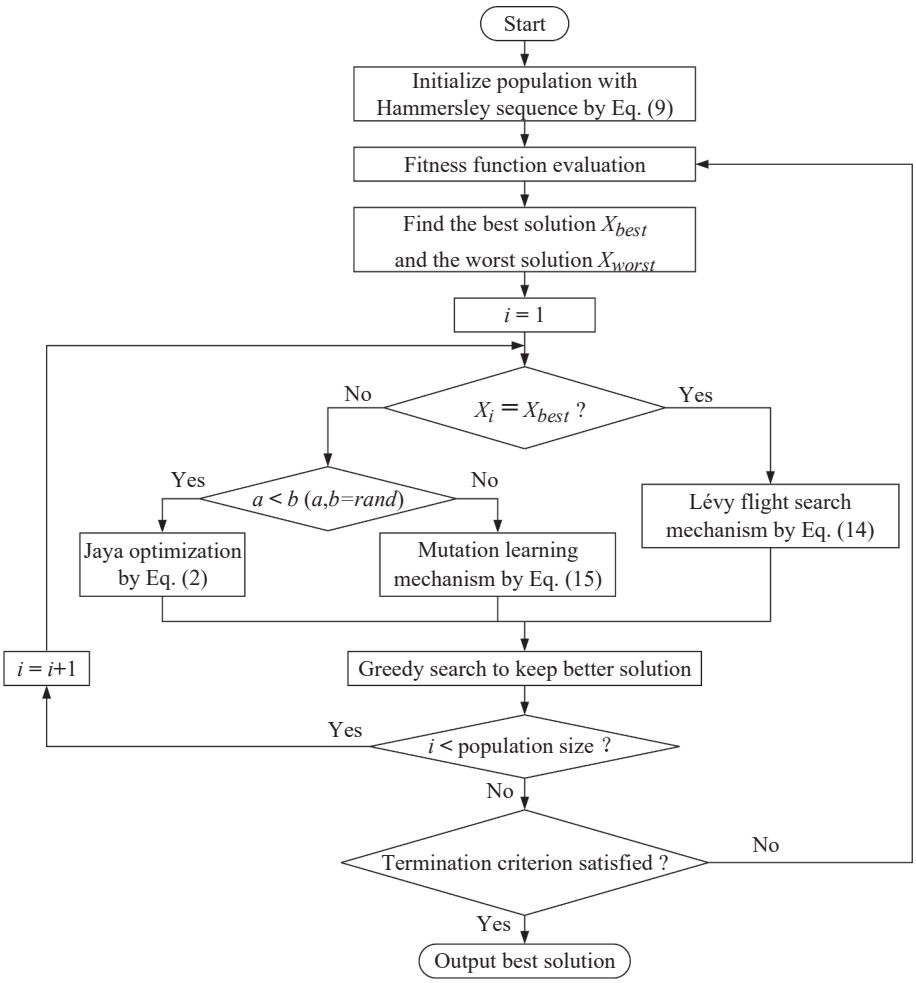

Fig. 3. The flowchart of proposed HJDEA.

3. Correlation function for damage identification

Correlation functions of dynamic responses can be used to identify structural damages. In this section, fitness function is established based on the adjacent acceleration correlation function, which is optimized by the proposed HJDEA. Hence, an output-only structural damage identification method using HJDEA and adjacent acceleration correlation function is developed.

3.1. Adjacent acceleration correlation function

The dynamic equation of linear elastic system with multiple degrees of freedom (MDOF) can be described as.

$$M\ddot{x}(t) + C\dot{x}(t) + Kx(t) = BF(t) \tag{16}$$

where M, C and K stand for the mass matrix, damping matrix and stiffness matrix of the structural system, respectively; herein, the damping matrix is modelled as Rayleigh damping$C = \ a_1M + a_2K$, where a_1 and a_2 are two damping constants, determined by the damping ratios of first two modes;$x(t)$, $\dot{x}(t)$ and $\ddot{x}(t)$ represent the displacement, velocity and acceleration vectors;. $F(t)$ denotes the time-dependent ambient excitation, which is generally considered as white noise. B is a mapping vector with the value of 1 at the excitation location and 0 at others.

Assuming the initial displacement and velocity of structure is zero, the acceleration response at the μ-th DOF can be calculated by.

$$\ddot{x}_\mu(t) = \int_{-\infty}^{\infty} \ddot{h}_\mu(t-\tau)F(\tau)d\tau \tag{17}$$

where $\ddot{h}_\mu(t)$ denotes unit impulse response function, and it can be obtained by following Newmark method.

$$\begin{cases} M\ddot{h}(t) + C\dot{h}(t) + Kh(t) = 0 \\ h(0) = 0, \dot{h}(0) = M^{-1}B \end{cases} \tag{18}$$

The cross-correlation function of accelerations at the μ- th and ζ-th DOFs can be expressed as.

$$\begin{aligned} R_{\mu\zeta}(\tau) &= E\left[\ddot{x}_\mu(t)\ddot{x}_\zeta(t-\tau)\right] \\ &= \int_{-\infty}^{t}\int_{-\infty}^{t-\tau} \ddot{h}_\mu(t-\mu_1)\ddot{h}_\zeta(t-\tau-\mu_2) \times E(f(\mu_1)f(\mu_2))d\mu_1 d\mu_2 \end{aligned} \tag{19}$$

where μ_1 and μ_2 means small time interval.

The equation of $E(f(\mu_1)f(\mu_2)) = S\delta(\mu_1 - \mu_2)$ can be obtained when external excitation is assumed as white noise, where S and $\delta(\mu_1 - \mu_2)$ represent a constant and Dirac delta function, respectively.

Then, Eq. (19) can be simplified as.

$$R_{\mu\zeta}(\tau) = S\int_0^{+\infty} \ddot{h}_\mu(t)\ddot{h}_\zeta(t-\tau)dt = H_{\mu\zeta}(\theta)S \tag{20}$$

where$H_{\mu\zeta}(\theta) = \int_0^{+\infty} \ddot{h}_\mu(t)\ddot{h}_\zeta(t-\tau)dt$, $H_{\mu\zeta}(\theta)$ stands for the convolution of unit impulse response functions, and it is only associated with unknown structural parameters. Thus, the cross-correlation function of accelera-

tions $R_{\mu\varsigma}$ depends on structural parameters θ to be identified and a constant S.

If n accelerometers are embedded in the structure simultaneously, the adjacent acceleration correlation function R can be written as.

$$R = \left[R_{1,2}, R_{2,3}, \cdots, R_{n-1,n}\right] \tag{21}$$

3.2. Damage identification with HJDEA and correlation function

In this paper, to present more accurate structural damage model, a series of elemental index vectors $\alpha = (\alpha_1, \alpha_2, ..., \alpha_i, ...\alpha_{ne})$ and $\beta = (\beta_1, \beta_2, ..., \beta_i..., \beta_{ne})$ taken from the range of [0, 1] are employed to consider alterations of both stiffness and mass parameters. The global stiffness matrix K^d and mass matrix M^d of damaged structure can be expressed as.

$$K^d = \sum_{i=1}^{ne}(1-\alpha_i)K_i^{ele} \tag{22}$$

$$M^d = \sum_{i=1}^{ne}(1-\beta_i)M_i^{ele} \tag{23}$$

where K_i^{ele} and M_i^{ele} stand for the stiffness and mass matrix of the i-th element under intact state; ne means the total number of structural elements; α_i and β_i are the damage index corresponding to the i-th elemental stiffness and mass. It is obvious that $\alpha_i = 0$ and $\beta_i = 0$ imply the i-th element is intact while $\alpha_i = 1$ and $\beta_i = 1$ represent this element is completely damaged. Therefore, structural parameters are$\theta = \{(1-\alpha_1), ..., (1-\alpha_{ne}), (1-\beta_1), ..., (1-\beta_{ne})\}$, and the problem of structural damage identification based on proposed damage model can be transformed into identifying damage index vectors α and β.

The proposed damage identification strategy based on HJDEA and correlation function is implemented as following steps:

Step 1: measure or calculate the actual acceleration response of damaged structure with pre-installed accelerometers under white noise excitation, and then obtain the measured adjacent acceleration correlation functions R_{mea}.

Step 2: Initialize the structural parameters θ in the search space limits with the Hammersley sequence.

Step 3: for each estimated structural parameters θ_i, calculate H_{est} and S_{est} with the equations of $H_{est}(\theta_i) = \int_0^{+\infty} \ddot{h}_\mu(t)\ddot{h}_\varsigma(t-\tau)dt$ and $S_{est} = \left(H_{est}^T H_{est}\right)^{-1} H_{est}^T R_{mea}$, and then compute the estimated correlation function R_{est} of the parameterized model by Eq. (20).

Step 4: Calculate the fitness function *fitness* based on measured and estimated cross-correlation functions as follows.

$$fitness = \frac{1}{c + \sum_{i=1}^{n-1}\sum_{j=1}^{l}\frac{|R_{est}(i,j)-R_{mea}(i,j)|^2}{E\left(R_{mea}^2(i)\right)}} \tag{24}$$

where n and l represent the number of accelerometers and data points; $E\left(R_{mea}^2(i)\right) = \sum_{n=1}^{l} R_{mea}^2(i, j)/l$ denotes the mean squared value of the i-th measured cross-correlation functions; c is a constant, whose value is set as 0.001. Thus, the maximum value of fitness function is equal to 1000 when R_{est} agrees with R_{mea}.

Step 5: Find the best and worst solutions, and then iteratively update the structural parameters using proposed hybrid Jaya and differential evolution algorithm.

Step 6: Repeat Step 5 until the maximum number of iterations reached or other termination conditions satisfied, and output the optimal identified structural parameters.

4. Numerical studies

To verify the identification accuracy, computational efficiency and noise robustness of the proposed output-only structural damage identification method based on the proposed HJDEA and correlation function, two numerical examples, namely an 8-floor shear-type frame and a cantilever beam subjected to white noise excitation are utilized. Specifically, the superiority of the proposed HJDEA is validated and compared with GA, PSO, Jaya algorithm in the first example. The effectiveness of proposed adjacent acceleration correlation function is tested and compared with reference point predefined method in the second example.

Algorithm parameters of GA and PSO are recommended from Refs. [18] and [50], respectively. The adopted parameters of GA, PSO, Jaya and HJDEA are listed in Table 2. The average value based on five runs is applied into performance evaluation to guarantee the effectiveness of identification results.

4.1. Comparison of four optimization algorithms

An 8-story shear-type steel frame structure from literature [14] is shown in Fig. 4(a), and its total height and width are 2000 mm and 600 mm, respectively. The width and thickness of identical steel beams are 100 mm and 25 mm, and the rectangular section of steel column is 50 × 5 mm. The initial elastic modulus of steel material is set as 2.0×10^{11}N/m^2, and the mass density is 7850 kg/m^3. The steel column and beam are welded together, and the bottom boundary condition is considered as fixed support. Thus, this frame structure can be modelled as an 8-DOF lumped mass model, as presented in Fig. 4(b), owing to its mass mainly concentrated on the beam. A white noise excitation with zero mean and unit standard deviation is horizontally applied to the top floor. As highlighted with red circle, four accelerometers located at the 1st, 3rd, 5th and 7th floor are used to record acceleration responses in horizontal direction with sampling frequency of 200 Hz and sampling duration of 1800 s. Adjacent acceleration correlation functions, namely $R_{1,3}$, $R_{3,5}$ and $R_{5,7}$, are used for damage identification.

Assuming 30% and 20% stiffness are reduced at elements 2 and 7 respectively, and 30% mass is reduced at element 4, namely $\alpha_2 = 0.3$, $\alpha_7 = 0.2, \beta_4 = 0.3$ White Gaussian noise is introduced into clean acceleration responses $\ddot{x}_{clean}$ to investigate the robustness of proposed structural identification strategy as follows.

$$\ddot{x}_{mea} = \ddot{x}_{clean} + N_l N_{noise} RMS\left(\ddot{x}_{clean}\right) \tag{25}$$

where $\ddot{x}_{mea}$ denotes noise-polluted measurement; N_l means the level of noise pollution; N_{noise} stands for the randomly generated noise vector of Gaussian distribution with zero mean and unit standard deviation; $RMS\left(\ddot{x}_{clean}\right)$ represents the root mean square of the acceleration response.

Fig. 5 and Table 3 present the convergence curves of fitness function and comparison of computational efficiency for four different algorithms, namely GA, PSO, Jaya and HJDEA, respectively. By Fig. 5, it can be clearly observed that GA and PSO provide relatively slow

Table 2
Parameters of GA, PSO, Jaya and HJDEA in numerical studies.

Parameters	GA	PSO	Jaya	HJDEA
Population size *NP*	100	100	60	60
Maximum generation G_m	400	400	200	200
Mutation probability P_m	0.2			
Crossover probability P_c	0.8			
Inertia weight w		decrease linearly from 0.9 to 0.4		
Cognitive parameter $c1$		2		
Social parameter $c2$		2		
Total evaluations	40,000	40,000	12,000	12,000

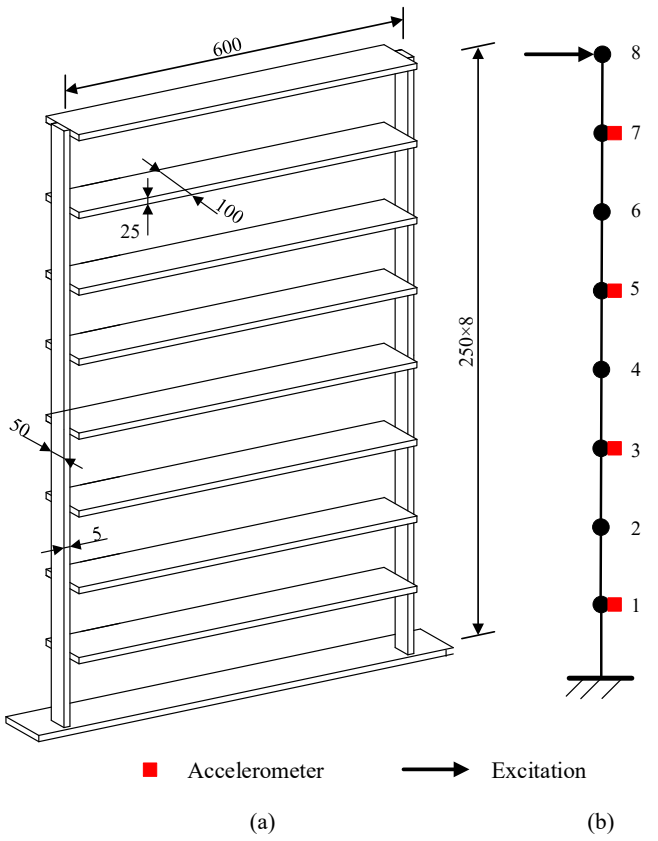

Fig. 4. The eight-floor steel frame structure: (a) dimension; (b) finite element model (unit: mm).

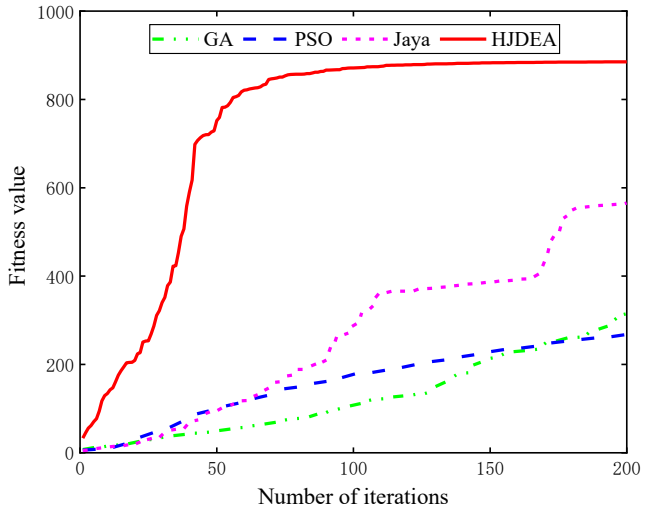

Fig. 5. Convergence process of fitness function for the frame structure.

Table 3
Comparison of computational efficiency for four different algorithms.

Methods	Fitness	Evaluations	Time for single evaluation (s)	Computational time (s)
GA	314.42	40,000	0.0174	697.12
PSO	267.74	40,000	0.0222	889.24
Jaya	565.60	12,000	0.0181	220.45
HJDEA	885.21	12,000	0.0178	215.16

convergence rate and inferior value of fitness. Similarly, Jaya also suffers by the unfavorable convergence speed because of its weak global search capacity in the early stage. In contrary, HJDEA approaches to convergence only around 100 iterations but achieves the best performance among four methods due to the successful combination of powerful global search capacity of DE and local search capacity of Jaya algorithm. As shown in Table 3, the calculated fitness of GA, PSO, Jaya and HJDEA are 314.42, 267.74, 565.60 and 885.21 respectively. The total computation time of GA and PSO are 697.12 s and 889.24 s, which is apparently longer than 220.45 s and 215.16 s consumed by Jaya and HJDEA. These results imply that HJDEA can obtain better fitness with less computational time compared with GA, PSO, and Jaya. Nevertheless, extensive number of iterations are still needed for HJDEA after the nearby location of optimal solution is approached, which would waste considerable computational resources. For this issue, an appealing method by combining HJDEA and gradient search is proposed to further improve identification efficiency, which will be deeply elaborated and discussed in Section 6.

Damage identification results of steel frame model based on four different algorithms are shown in Figs. 6 and 7 for noise free and 20% noise case, respectively. In addition, the identified errors of stiffness and mass parameters based on average value over five runs are provided in Table 4, and identification results of damaged elements are listed in Table 5. It can be observed from Fig. 6 that GA and PSO are able to detect locations of the damaged element, but they cannot accurately identify damage extent, and several false identifications are evidently observed at elements 1, 3, 5, 6 and 8. As listed in Table 4, the maximum identification errors of structural parameters based on GA and PSO are 12.37% and 13.69% for noise free case, which means these two algorithms fail to identify stiffness and mass parameters. On the contrary, Jaya and HJDEA are able to provide accurate identification results of damage existence, location and severity, with less than 4% and 2% for the maximum errors respectively. Besides, in Table 5, it can be found that the identified standard deviations of α_2, α_7, β_4 by HJDEA are apparently smaller than Jaya. Thus, these results indicate that proposed hybrid algorithm has higher identification accuracy and stronger robustness. For the case with 20% noise contaminated, GA and PSO obtain unacceptable results with the maximum errors more than 16% and some obvious false identification at elements 1, 2, 3, 4, 6, and 8. Although the locations of the damaged element are successfully identified, Jaya has difficulty in estimating the damage extent of mass parameter at element 4. Large relative error of 33.91% and standard deviation of 0.179 are obtained. Among four algorithms, HJDEA achieves the best performance with maximum standard deviation less than 0.015 and maximum error of structural parameters less than 5% even with 20% noise pollution. These excellent results demonstrate that the proposed HJDEA is effective and robust to simultaneously identify the reduction of elemental stiffness and mass using output-only responses by optimizing the objective function based on adjacent acceleration correlation function.

Another possible damage case is considered to further validate the robustness of the proposed method. Assuming 20%, 15% stiffness are reduced at elements 2, 6 respectively, and 20%, 15% mass are reduced at elements 3 and 5, namely $\alpha_2 = 0.20$, $\alpha_6 = 0.15$, $\beta_3 = 0.20$, $\beta_5 = 0.15$. The calculated fitness value and computational time for these four algorithms are listed in Table 6. It can be observed form Table 6 that the calculated fitness value of GA, PSO, Jaya and HJDEA are 334.13, 289.43, 586.62 and 899.24 respectively. The total computation time of GA and PSO are 700.56 s and 880.47 s, which is obviously larger than 219.95 s and 218.64 s taken by Jaya and the proposed HJDEA method. These results indicate HJDEA can achieve high fitness value but consumed less computational time compared with GA, PSO, and Jaya.

In addition, identification accuracy of stiffness and mass parameters for GA, PSO, Jaya, HJDEA is studied and presented in Table 7. For the noise free case, the maximum errors of the identified parameters based on GA and PSO are 10.48% and 12.02%, and such a poor result indicates

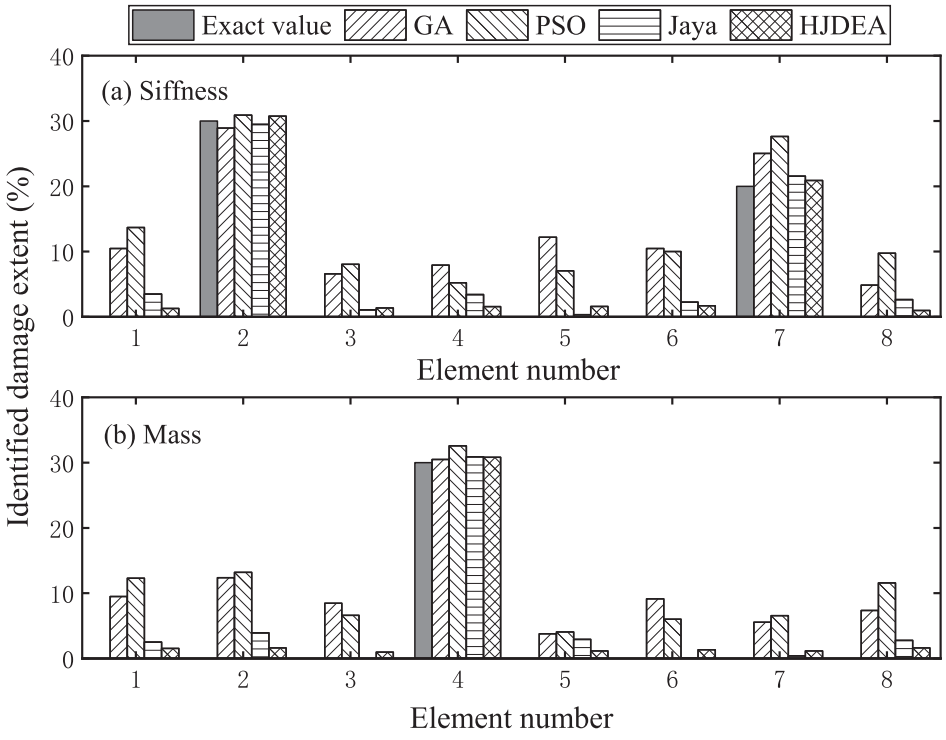

Fig. 6. Damage identification results of steel frame without noise: (a) stiffness; (b) mass.

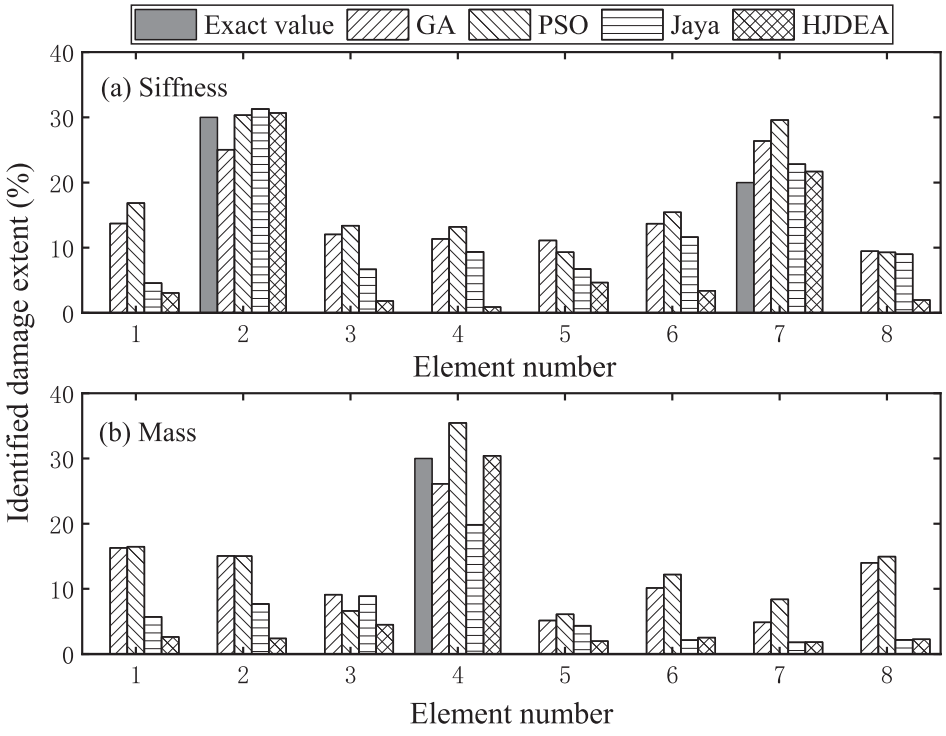

Fig. 7. Identified damage extent with 20% noise: (a) stiffness; (b) mass.

that these two algorithms fail to accurately identify structural parameters. In contrast, Jaya and HJDEA can provide more pleasant identification results of damage location and extent with less than 4% and 2% maximum errors, respectively. For the 20% noise case, apparently unacceptable results with the maximum errors of more than 13% and 16% are obtained by GA and PSO, respectively. On the contrary, HJDEA achieves quite favorable results with the maximum and mean errors of less than 4.5% and 2.5%. These results demonstrate that the proposed HJDEA has more effective and robust performance than GA, PSO, Jaya to simultaneously identify stiffness and mass parameters even with 20% noise polluted responses.

Table 4
Identified errors for four different methods (%).

Errors	Noise free				20% noise			
	GA	PSO	Jaya	HJDEA	GA	PSO	Jaya	HJDEA
Mean error-*K*	7.32	7.79	1.92	1.18	10.33	10.92	6.51	2.27
Max error-*K*	12.19	13.69	3.50	1.70	13.72	16.85	11.63	4.64
Mean error-*M*	7.08	7.86	1.70	1.28	9.80	10.65	5.37	2.31
Max error-*M*	12.37	13.19	3.93	1.63	16.28	16.46	10.17	4.51

Table 5
Identified results of damage elements for the steel frame.

Methods	Damage extent	Noise-free			20% noise		
		Mean value	RE (%)	SD	Mean value	RE (%)	SD
GA	$\alpha_2 = 0.3$	0.2892	3.61	0.053	0.2502	16.59	0.069
	$\alpha_7 = 0.2$	0.2002	25.09	0.027	0.2636	31.82	0.038
	$\beta_4 = 0.3$	0.3049	1.63	0.035	0.2611	12.97	0.054
PSO	$\alpha_2 = 0.3$	0.3089	2.96	0.045	0.3032	1.07	0.017
	$\alpha_7 = 0.2$	0.2763	38.16	0.036	0.2959	47.95	0.047
	$\beta_4 = 0.3$	0.3257	8.56	0.039	0.3546	18.19	0.046
Jaya	$\alpha_2 = 0.3$	0.2947	1.76	0.014	0.3128	4.27	0.036
	$\alpha_7 = 0.2$	0.2155	7.76	0.021	0.2282	14.08	0.094
	$\beta_4 = 0.3$	0.3089	2.98	0.051	0.1983	33.91	0.179
HJDEA	$\alpha_2 = 0.3$	0.3073	2.42	0.005	0.3066	2.20	0.008
	$\alpha_7 = 0.2$	0.2089	4.43	0.010	0.2169	8.46	0.012
	$\beta_4 = 0.3$	0.3081	2.70	0.014	0.3040	1.34	0.013

Note: RE means relative error and SD stands for standard deviation.

Table 6
Comparison of fitness and computational time for GA, PSO, Jaya, HJDEA.

Methods	Fitness	Evaluations	Time for single evaluation (s)	Computational time (s)
GA	334.13	40,000	0.0175	700.56
PSO	289.43	40,000	0.0220	880.47
Jaya	586.62	12,000	0.0183	219.95
HJDEA	899.24	12,000	0.0182	218.64

4.2. Comparison of reference point free and defined method

Reference point is necessarily defined as reviewed in previous literatures [11–14]. However, damage identification result may be affected by the selection of reference point. The proposed adjacent acceleration correlation function in Section 3.1 is a reference point-free method, and its performance is compared with reference point predefined method on the damage identification accuracy and robustness in this section. The previous numerical study has demonstrated that HJDEA outperforms the other three swarm intelligence optimization algorithms in terms of identification accuracy and computational efficiency, so only hybrid

Table 7
Identified errors of stiffness and mass parameters for GA, PSO, Jaya, HJDEA (%).

Errors	Noise free				20% noise			
	GA	PSO	Jaya	HJDEA	GA	PSO	Jaya	HJDEA
Mean error-*K*	6.58	7.66	1.98	1.19	9.71	10.17	6.26	2.24
Max error-*K*	10.48	12.02	3.93	1.84	13.72	15.43	9.63	4.40
Mean error-*M*	6.70	7.11	1.75	1.23	8.99	9.92	5.49	2.26
Max error-*M*	9.50	11.57	3.97	1.62	13.98	16.63	8.88	4.12

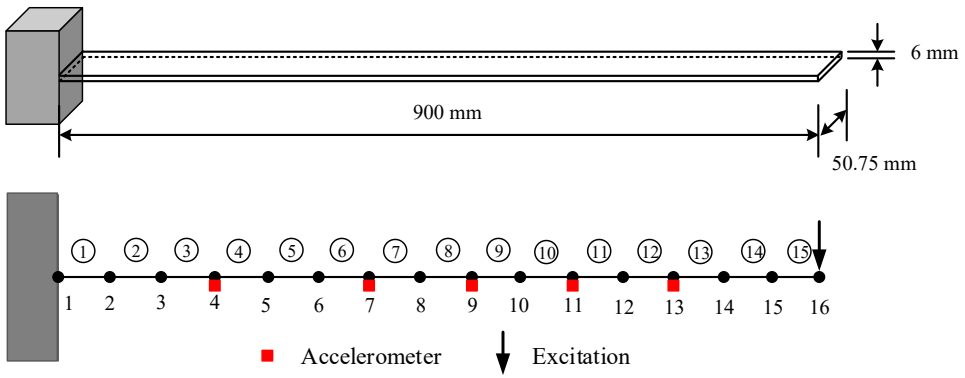

Fig. 8. Numerical model of a cantilever beam structure.

algorithm is utilized for the following studies. A cantilever beam structure with more element numbers is employed as numerical example to better present the superiority of proposed reference point-free method.

As presented in Fig. 8, the total length, section width and height of cantilever beam are 900 mm, 50.75 mm and 6 mm, respectively. Due to the large ratio of length to height, shear strain is not considered according to the Euler-Bernoulli beam theory. The finite element model of the cantilever beam has total numbers of 16 nodes and 15 elements, and each element has identical length of 60 mm. Each node has two degrees of freedom, i.e., vertical translation and rotation. The material of cantilever beam is steel with the elastic modulus of $2.1 \times 10^{11}\mathrm{N/m^2}$ and the mass density of 7860 $\mathrm{kg/m^3}$. From Fig. 8, it is observed that a white noise excitation with zero mean and unit standard deviation is vertically applied at node 16. A more difficult yet practical case of partial measurements is employed to identify structure damage. Five accelerometers are installed at nodes 4, 7, 9, 11, and 13 to record the dynamic response of the cantilever beam structure in vertical direction with sampling frequency of 2000 Hz and sampling duration of 1800 s.

To simulate more complex and reasonable damage cases including multiple damages or both stiffness and mass related damages, it is assumed that there are 20% and 15% reduction of stiffness at the 3rd and 12th elements, 20% and 10% reduction of mass at the 6th and 9th elements, which means damage indexes $\alpha_3 = 0.2, \alpha_{12} = 0.15, \beta_6 = 0.2$, $\beta_9 = 0.1$ respectively. To evaluate the effectiveness of the proposed reference point-free method (RP_0), adjacent acceleration correlation functions, namely $R_{4,7}$, $R_{7,9}$, $R_{9,11}$, $R_{11,13}$, are calculated, and its computational results are compared with reference point-defined methods, taking measurement at node 4, 7, 11 as the reference points (RP_4, RP_7, RP_{11}) respectively. In this example, first 200 data points of the cross-correlation functions are selected for damage identification. The damage identification results of the cantilever beam structure under the noise free and 20% noise polluted conditions are shown in Figs. 9 and 10, respectively. Table 8 lists the statistical maximum and mean identified errors.

For the case of noise free, it can be seen from Fig. 9 that RP_4 provides the worst identification results among the four different methods. Some unneglected identification errors are easily observed at the elements 7, 8, 10 and 11, and the maximum errors of stiffness and mass are more than 14 % and 13%, respectively, which means RP_4 has some difficulties in identifying the location and extent of structural damage. On the contrary, reference point-defined method RP_{11} can accurately identify the damage location and degree with the maximum errors of stiffness and mass parameters of less than 1.5% and 3.5%, as well as the mean errors less than 0.6% and 0.9%, respectively. Obviously, pleasant results of RP_0 can be found in the Fig. 9 and Table 8. There is no apparent false identification and the identified mean errors of stiffness and mass are less than 0.6% and 1.1%. When contaminated with 20% noise, RP_4 also fails in identifying structural damages with the poor identification result of maximum error up to 27.45%. Although the damage location and extent are successfully identified by RP_7, several apparent false identifications occur at the elements 2, 6, 10 and 15. Among the four methods, RP_{11} acquires the most satisfactory identification results with the mean errors of 1.03% and 1.06%. From above description, it can be found that selection of different reference points would dramatically affect the computational results. Improper reference point will result in unacceptable identification results. On the contrary, the proposed RP_0 method is more robust to identify multiple structural damage with maximum errors of 5.66% and 6.41% for stiffness and mass related damages, respectively. This result is acceptable taking the limited sensors and 20% noise polluted measurements into account.

Another possible damage case is considered to further validate the robustness of the proposed reference point free method. It is assumed that there are 20%, 15%, 10% reduction of stiffness at the 3rd, 8th 13th elements, 20%, 15%%, 10% reduction of mass at the 6th, 9th, 12th elements, which means damage indexes $\alpha_3 = 0.20$, $\alpha_8 = 0.15$, $\alpha_{13} = 0.10$, $\beta_6 = 0.20$, $\beta_9 = 0.15$, $\beta_{12} = 0.10$, respectively. The identified results by four methods are presented in Fig. 11 and Fig. 12 corresponding to the noise free and 20% noise case, respectively. The maximum and mean identified errors are listed in Table 9.

For the noise-free case, it can be seen from Fig. 11 that RP_4 achieves the worst results with the maximum error of identified stiffness and mass parameters more than 12% among four different methods. Some obvious false identifications are observed at the elements 4, 5, 6 and 12, which indicates RP_4 has some difficulties in identifying structural damages.

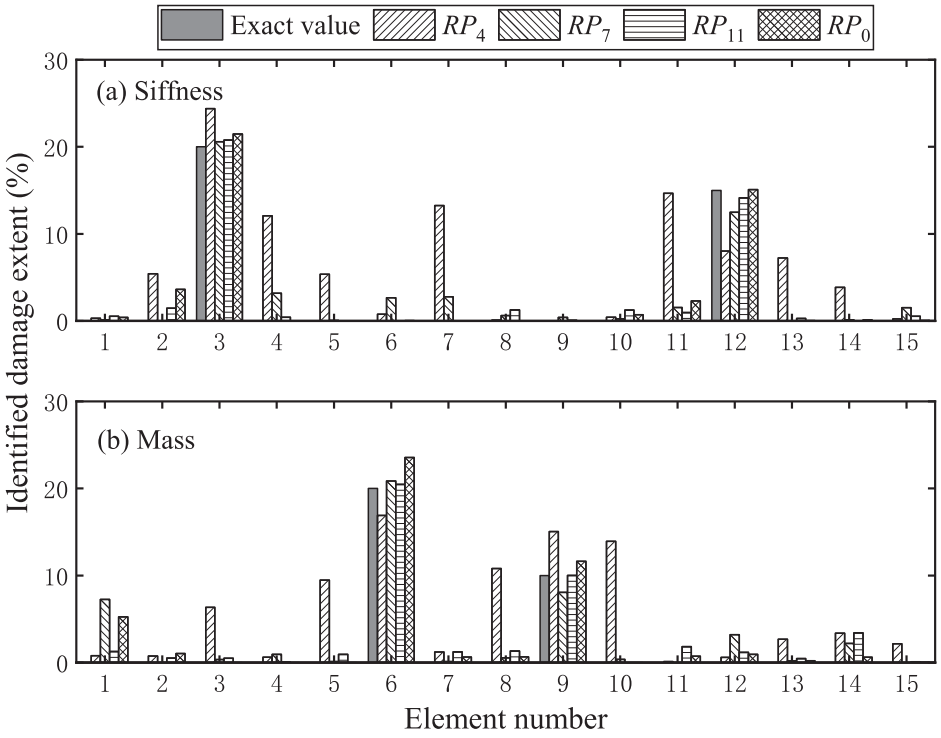

Fig. 9. Damage identification results of cantilever beam without noise: (a) stiffness; (b) mass.

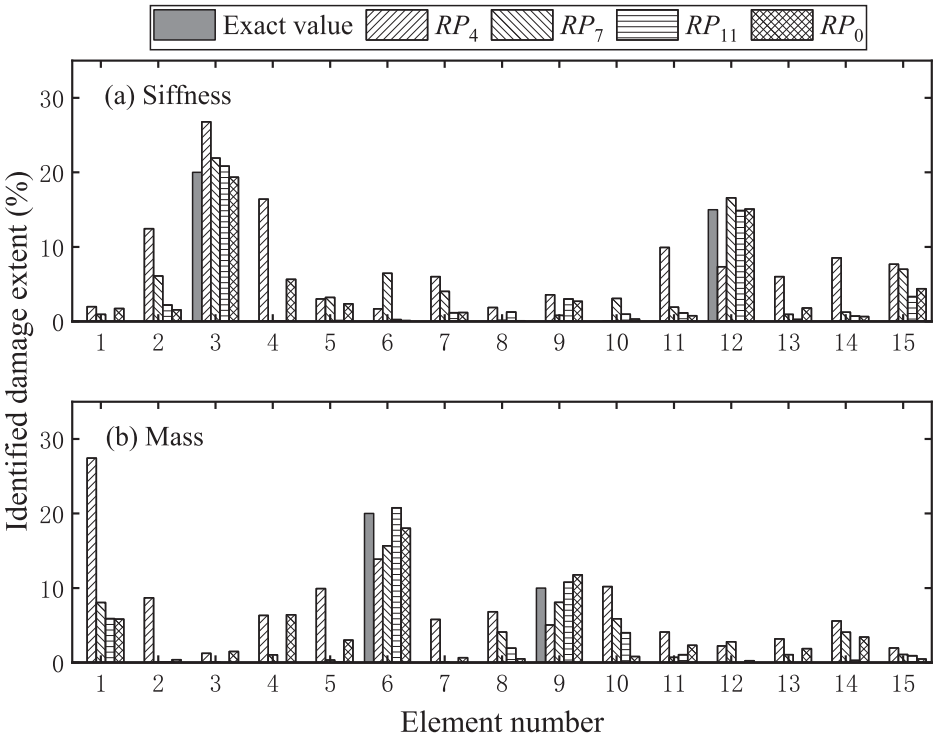

Fig. 10. Damage identification results of cantilever beam with 20% noise: (a) stiffness; (b) mass.

Table 8
Identification results of the stiffness and mass parameters (%).

Methods	Parameters	Noise free		20% noise	
		Maximum error	Mean error	Maximum error	Mean error
RP_4	Stiffness	14.66	5.01	16.45	6.24
	Mass	13.92	4.07	27.45	6.97
RP_7	Stiffness	3.18	1.09	7.00	2.63
	Mass	7.27	1.21	8.05	2.37
RP_{11}	Stiffness	1.46	0.56	3.33	1.03
	Mass	3.41	0.89	5.90	1.06
RP_0	Stiffness	3.62	0.59	5.66	1.60
	Mass	5.25	1.02	6.41	2.08

Although the damage location and extent are successfully identified by RP_7, apparent false identifications occur at the elements 1, 3, 10. RP_{11} can accurately identify the damage location and degree with the maximum errors of less than 2.0% and mean errors less than 0.8%, respectively. Favorable results are also obtained by the proposed RP_0. There is no apparent false identification and the identified maximum errors of stiffness and mass are less than 2.5%% and 3.0%. For 20% noise case, similarly, RP_4 fails to identify structural damages with the poor identification result of maximum error up to 17.21% and RP_{11} obtains more satisfactory results with the maximum and mean errors of 2.33% and 0.92% than other three methods. It can be found from Table 9 that selection of different reference points would dramatically affect the accuracy of identified results. In other words, selecting improper reference point may lead to unacceptable identification results. In contrast, the proposed reference point free method RP_0 is more robust to identify multiple structural damages with the maximum errors of 4.51% and 3.91% for stiffness and mass with 20% noise polluted measurements.

In summary, it can be concluded that the proposed method of adjacent acceleration correlation function has competitive or even better performance than those acquired by reference point-defined methods. More importantly, adjacent acceleration correlation function has the capacity of robustness to avoid the false identification results caused by selecting inappropriate reference points.

5. Experimental verifications

In the past two decades, researchers have conducted numerous theoretical and experimental studies on structural health monitoring, and proposed various damage identification methods. However, these works are basically suitable for different engineering structures or different application conditions, rending it difficult to compare and judge their effectiveness and robustness. With the purpose of providing a unified standard research platform for analysis, comparison and evaluation of different damage identification techniques, the IASC-ASCE SHM Benchmark structure was developed in the Earthquake Engineering Research Laboratory at the University of British Columbia (UBC) [51]. In this section, the applicability of the proposed method to structural damage identification is verified and compared with GA, PSO, Jaya algorithms with the ASCE Benchmark structure. As presented in Fig. 13 [52], the scale-model is a 4-story, 2- bay by 2-bay steel frame. It has plan dimension of 2.5 m × 2.5 m and total height of 3.6 m. Each floor has 8 identical braces. The detailed properties of structural members are listed in Table 10. This ASCE Benchmark model is made of hot rolled 300 W grade steel with a nominal yield strength of 300 MPa, and its elastic modulus and mass density are 2.0 × 10^{11}N/m^2 and 7800 kg/m^3, respectively.

A linear 12 degree-of-freedom shear model subjected to white noise excitation on the roof is employed, and 4 accelerometers are installed at each story to record the structural response with sampling frequency of 500 Hz and sampling duration of 1800 s. Herein, acceleration cross-correlation functions of the 1st and 2nd floors ($R_{1,2}$), the 2nd and 3rd floors ($R_{2,3}$), the 3rd and 4th floors ($R_{3,4}$), are employed for structural damage identification. The horizontal stiffness of health structure in the strong (x) direction and weak (y) direction are 106.60 MN/m and 67.90 MN/m in each story. As listed in Table 11, four different damage patterns are considered to test the capacity of cross-correlation function-based method for identifying damage existence, location and severity. Damages are introduced by removing braces. There are only less than

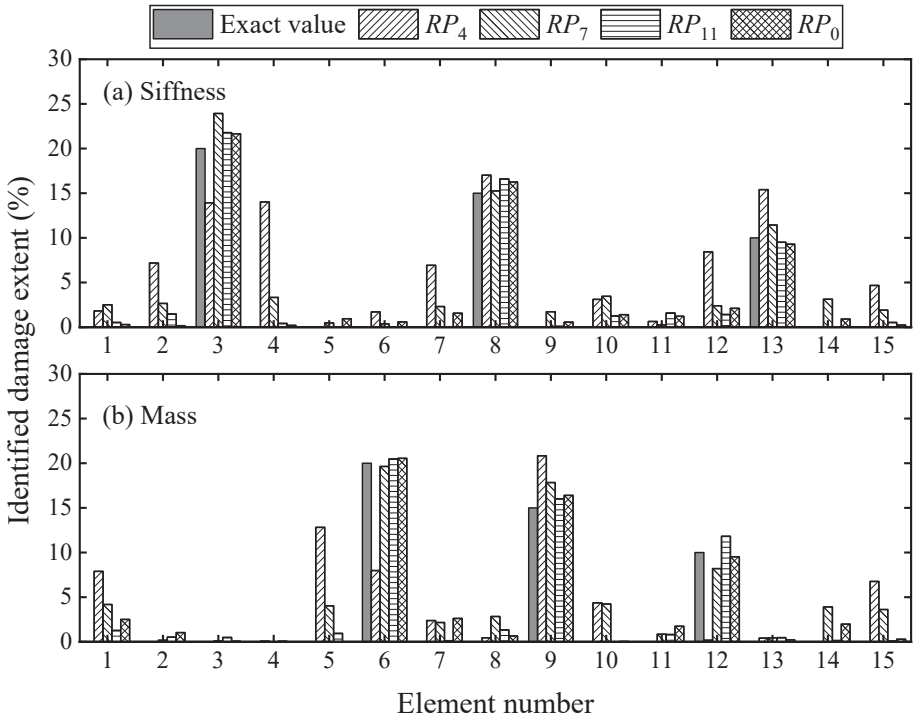

Fig. 11. Identified results for RP_4, RP_7, RP_{11}, RP_0 without noise: (a) stiffness; (b) mass.

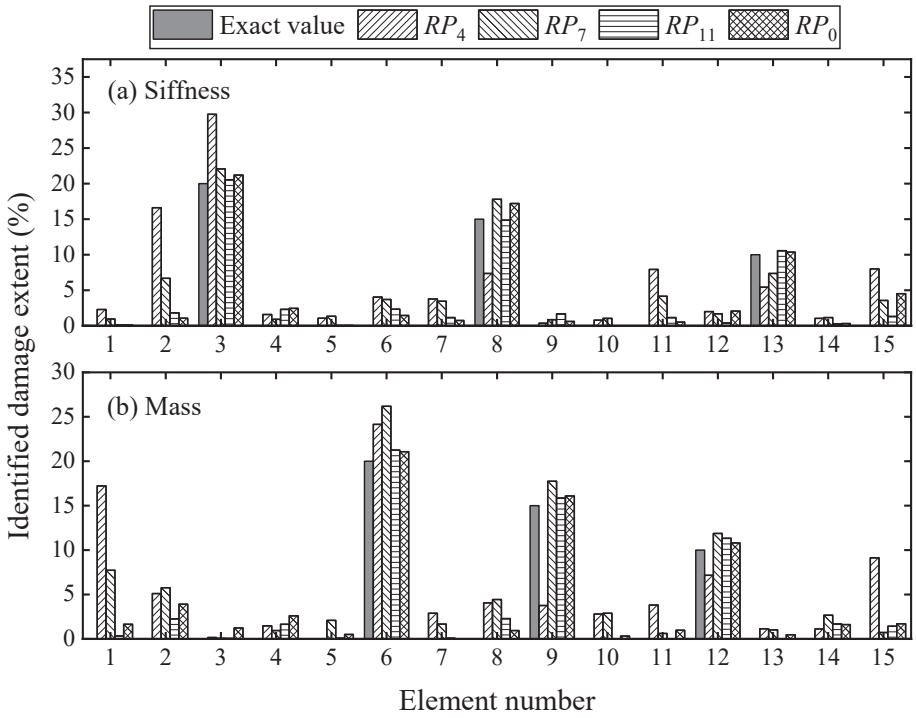

Fig. 12. Identified results for RP_4, RP_7, RP_{11}, RP_0 with 20% noise: (a) stiffness; (b) mass.

1% alteration of element mass in these four damage patterns. Thus, damage indexes of mass parameters are assumed to be $\beta_i = 0$ in this example. The same algorithms parameters for GA, PSO, Jaya listed in Table 2 are adopted in this experimental study. HJDEA is employed to detect four damage patterns with the parameter settings of population size 60 and maximum generation 100. The corresponding results of stiffness and mass parameters by GA, PSO, Jaya and HJDEA are presented in Fig. 14 and Table 12.

It can be obviously observed from Fig. 14 that GA, PSO, Jaya and HJDEA with adjacent acceleration correlation function are capable of accurately identifying the damage location and extent. The maximum error obtained by these four methods is less than 5.5%. Especially, the identified structural stiffness and mass parameters by proposed HJDEA match very well with the exact values for these four damage patterns, e.g., the maximum errors of stiffness are 1.71%, 1.05%, 0.81%, 1.14%, and the maximum errors of mass are 1.64%, 1.39%, 2.39%, 1.38%,

Table 9
Identification results for RP_4, RP_7, RP_{11}, RP_0 (%).

Methods	Parameters	Noise free		20% noise	
		Maximum error	Mean error	Maximum error	Mean error
RP_4	Stiffness	14.02	4.13	16.62	4.77
	Mass	12.82	4.19	17.21	4.47
RP_7	Stiffness	3.93	2.01	6.69	2.47
	Mass	4.24	2.10	7.73	2.76
RP_{11}	Stiffness	1.77	0.74	2.33	0.92
	Mass	1.82	0.64	2.29	0.89
RP_0	Stiffness	2.12	0.92	4.51	1.18
	Mass	2.63	0.91	3.91	1.26

respectively, which is fairly satisfying under the conditions with output-only responses and no priori knowledge of mass and stiffness. These results demonstrate the proposed HJDEA can more accurately and efficiently identify damage location and severity than GA, PSO, Jaya algorithm under multiple damage situations.

Fig. 15 presents the convergence history of identified damage elements for damage pattern 2 and 4 by the proposed HJDEA method. It is noted that HJDEA takes around 30 iterations to approximately converge to the damage extent, namely $\alpha_{1\_x} = 45.24\%$, $\alpha_{1\_y} = 71.03\%$, $\alpha_{3\_x} = 45.24\%$, $\alpha_{3\_y} = 71.03\%$ for damage pattern 2 and $\alpha_{1\_y} = 17.76\%$, $\alpha_{3\_x} = 11.31\%$ for damage pattern 4. These results clearly imply that the proposed hybrid identification method is capable of accurately and efficiently identifying damage location and degree.

Furthermore, a comparison of cross-correlation function between healthy state and damage state of pattern 3 is conducted, provided in Fig. 16, to show the effectiveness of cross-correlation function for damage identification. There are three cross-correlation functions of adjacent acceleration from four measurements $R_{1,2}$, $R_{2,3}$ and $R_{3,4}$, and first 300 data points of adjacent acceleration correlation function are presented in Fig. 16. It is observed that the cross-correlation function in healthy state R_{hea} deviates from measured or estimated value in damage state, which implies adjacent acceleration correlation function is a sensitive index to reflect damage. In addition, the measured cross-correlation function R_{mea} agrees well with the estimated cross-correlation functionR_{est}. Herein, relative error (*RE*) and Pearson correlation coefficient (*PCC*) are utilized to measure the deviation and linear correlation degree between the measured and estimated value as follows.

$$RE = \frac{\|R_{est} - R_{mea}\|_2}{\|R_{mea}\|_2} \times 100\% \tag{26}$$

$$PCC(R_{mea}, R_{est}) = \frac{Cov(R_{mea}, R_{est})}{\sigma_{R_{mea}} \sigma_{R_{est}}} \tag{27}$$

where: *Cov* stands for covariance; σ means standard deviation.

Computational results with $RE = 13.37\%$ and $PCC = 0.9918$ demonstrates that HJDEA is able to effectively identify structural damage by optimizing the fitness function established by measured and estimated cross-correlation functions.

6. Discussion

As described in Section 4.1, considerable number of fitness

Table 10
Physical properties of Benchmark structure.

Property	Braces	Beams	Columns
Section type	L25 × 25 × 3	S75 × 11	B100 × 9
Cross-section area A (m^2)	0.141×10^{-3}	1.43×10^{-3}	1.133×10^{-3}
Moment of inertia(strong) I_x (m^4)	0	1.22×10^{-6}	1.97×10^{-6}
Moment of inertia(weak) I_y (m^4)	0	0.249×10^{-6}	0.664×10^{-6}
Torsion constant J (m^4)	0	38.2×10^{-9}	8.01×10^{-9}
Shear modulus G (Pa)	0.77×10^{11}	0.77×10^{11}	0.77×10^{11}

Table 11
Four different damage patterns.

Patterns	Damage location	Specific damage	Damage extent
1	1st story	Remove all braces	$\alpha_{1\_x} = 0.4524, \alpha_{1\_y} = 0.7103$
2	1st and 3rd stories	Remove all braces	$\alpha_{1\_x} = 0.4524, \alpha_{1\_y} = 0.7103$ $\alpha_{3\_x} = 0.4524, \alpha_{3\_y} = 0.7103$
3	3nd story	Remove one brace	$\alpha_{1\_y} = 0.1776$
4	1st and 3rd stories	Remove one brace in each story	$\alpha_{1\_y} = 0.1776, \alpha_{3\_x} = 0.1131$

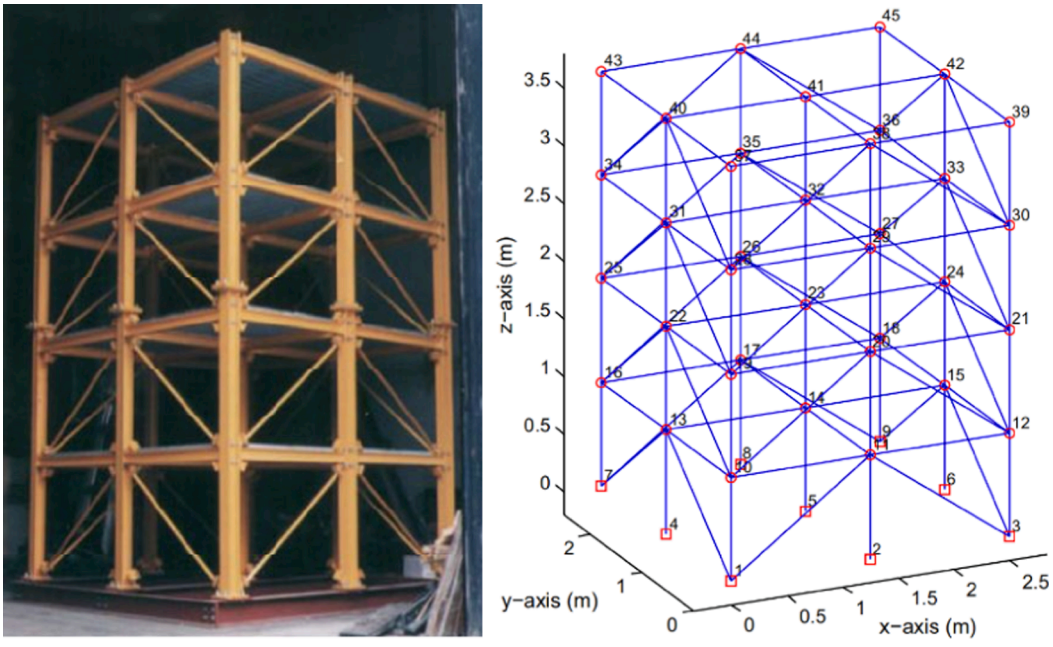

Fig. 13. Experimental model of ASCE Benchmark structure.

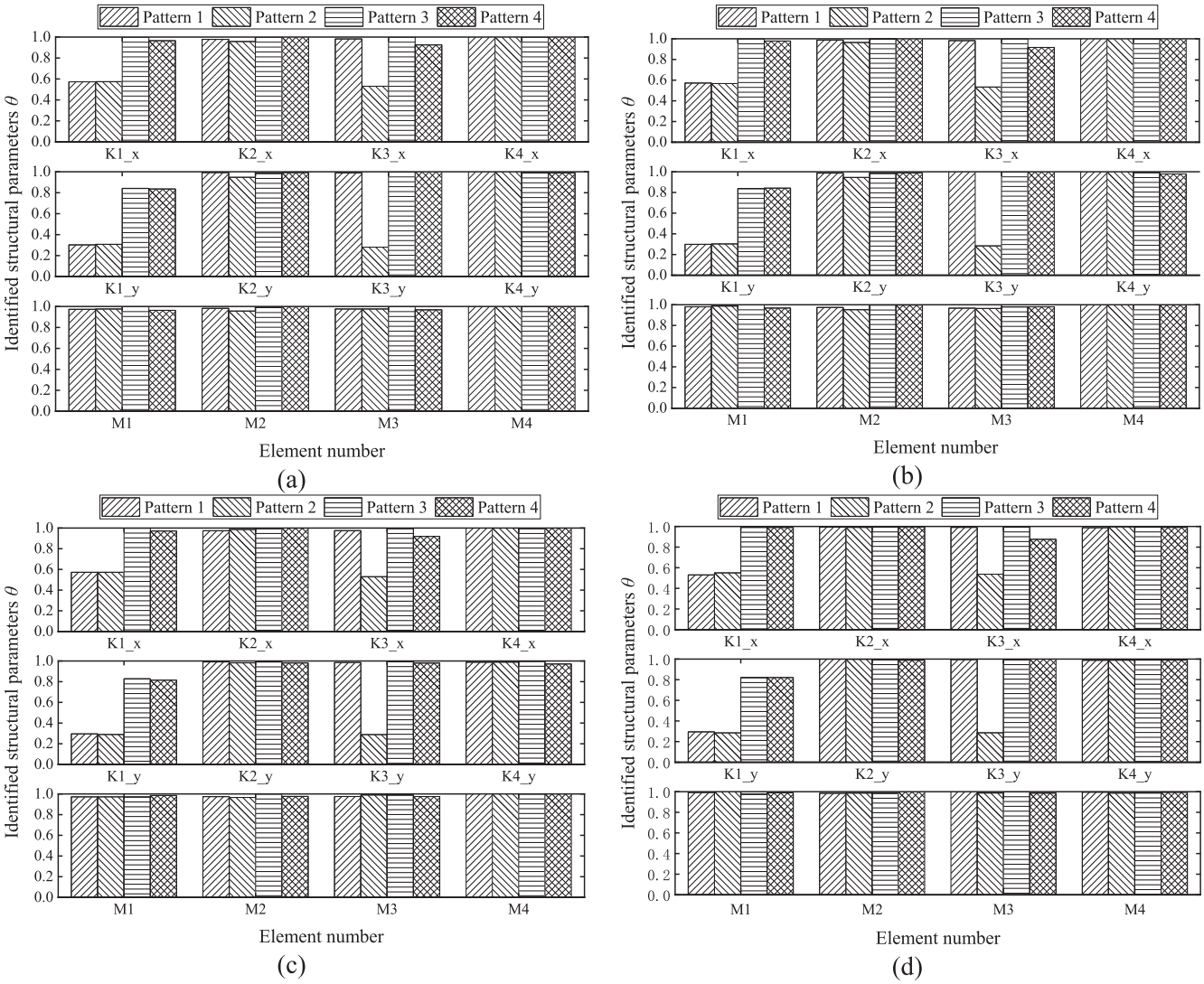

Fig. 14. Identified results of stiffness and mass parameters with: (a) GA; (b) PSO; (c) Jaya; (d) HJDEA.

Table 12
Identification error for four damage patterns with four different methods (%).

Methods	Identified error	Pattern 1	Pattern 2	Patter 3	Pattern 4
GA	Max error-*K*	2.57	5.25	1.91	3.82
	Max error-*M*	2.67	4.40	0.92	3.72
PSO	Max error-*K*	2.44	5.48	1.50	2.92
	Max error-*M*	3.23	4.78	2.00	3.18
Jaya	Max error-*K*	2.56	2.44	2.69	3.27
	Max error-*M*	2.79	3.37	2.85	2.46
HJDEA	Max error-*K*	1.71	1.05	0.81	1.14
	Max error-*M*	1.64	1.39	2.39	1.38

evaluations are still required for the proposed HJDEA even in a relatively small search space when the nearby location of optimal solution is approached, which would waste much computational resources to achieve pleasant damage identification results. In fact, HJDEA has strong search capacity in the early stage, while suffers from the relatively slow convergence rate due to the inherent stochastic optimization characteristic of population-based optimization algorithm. On the contrary, gradient search has higher computational efficiency and more powerful local search ability than HJDEA. Nevertheless, good initial guess is generally needed for gradient search method. Therefore, it would be a meaningful attempt to combine HJDEA and gradient search method with the attractive idea of roughly approaching to the optimal solution by HJDEA and then taking it as initial values in the subsequent gradient search to utilize its strong local search ability. The cantilever beam structure in Section 4.2 is taken as numerical example to investigate the hybrid HJDEA and gradient search method.

It is obvious from Fig. 17(a) that gradient search, initially approximating to the optimal solution after 30 iterations by HJDEA and then taking the identified value as initial guess in the subsequent gradient search, achieves larger fitness value than HJDEA only with 80 iterations in total. In addition, a more evident contrast can be observed by Fig. 17 (b). The total number of fitness function evaluations by hybrid HJDEA and gradient search is 2300, far less than 12,000 taken by HJDEA. Fig. 18 provides the detailed convergence history of fitness value and mean errors calculated by gradient search, in which the final results of fitness approximate to 1000 and mean error less than 1% are observed. The comparison of two methods presented in Table 13 shows that only extra 500 times of candidate evaluation are required after 1800 evaluations of HJDEA, while more favorable results in terms of smaller identification errors and less computational times are acquired, which indicates the combination of hybrid HJDEA and gradient search method is a feasible strategy to first achieve coarse global search by HJDEA to the position near the optimal solution, and then taking as initial value in gradient search for further refining the quality of identified results. Therefore, it can be concluded that hybrid HJDEA and local search

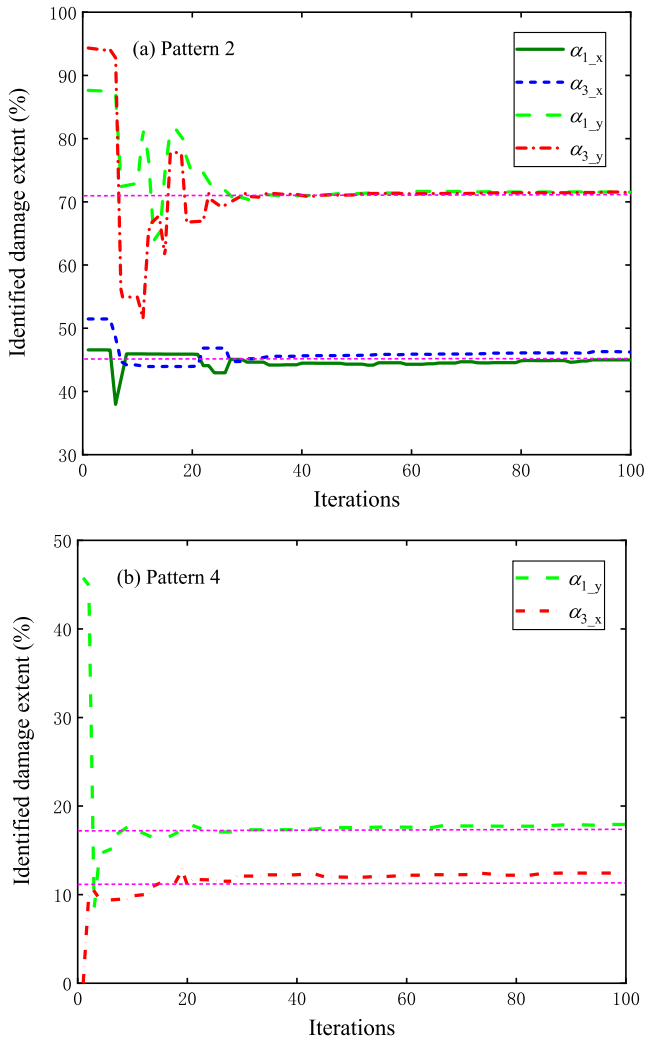

Fig. 15. The convergence history of identified damage elements: (a) damage pattern 2; (b) damage pattern 4.

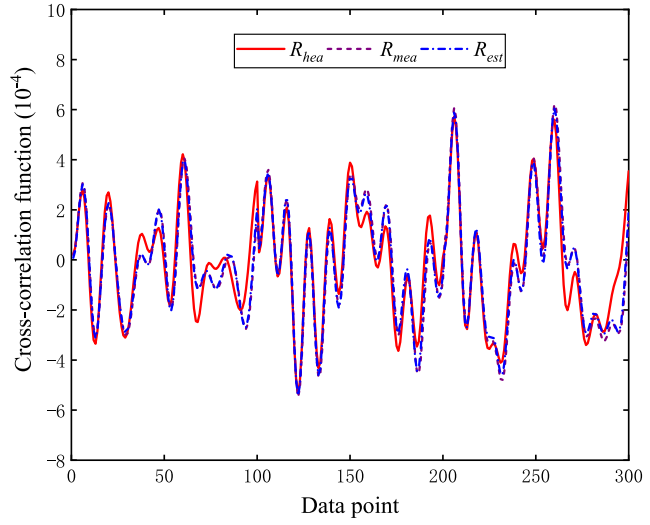

Fig. 16. Comparison of cross-correlation function between healthy state and damage pattern 3.

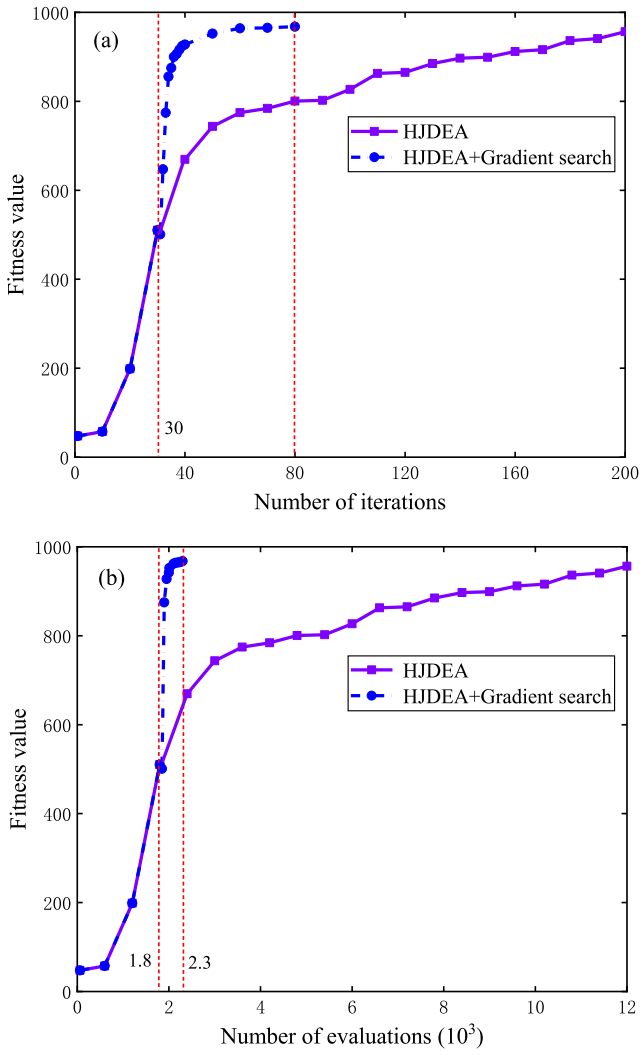

Fig. 17. Convergence history with: (a) number of iterations; (b) number of evaluations.

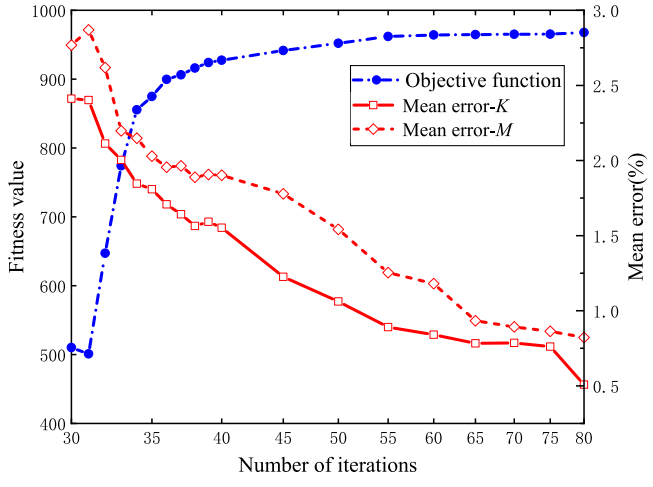

Fig. 18. Fitness and mean error of gradient search after 30 iterations with HJDEA.

Table 13
Comparison of HJDEA, hybrid HJDEA and gradient search method.

Method	Number of iterations	Number of evaluations	Fitness	Computational times (s)	Mean error (%)	
					Stiffness	Mass
JHDEA	200	12,000	956.43	510.73	0.65	0.95
HJDEA and gradient search	30	1800	510.21	76.54	2.41	2.78
	40	1900	927.45	106.48	1.55	1.90
	50	2000	952.06	135.56	1.06	1.54
	60	2100	964.18	165.78	0.84	1.18
	70	2200	965.16	194.86	0.78	0.89
	80	2300	965.71	224.98	0.51	0.82

methods is a promising alternative to further improve identification accuracy and computational efficiency.

7. Conclusions

In this paper, a hybrid algorithm based on Jaya and differential evolution algorithm is proposed with the purpose of effectively combining the powerful local search capability of Jaya and global search capability of differential evolution, to detect, locate and quantify the multiple structural damages. In the proposed hybrid algorithm, Hammersley sequence initialization and Lévy flight search mechanism are introduced to increase the diversity of initial population and refine the quality of identified best solution. Besides, adjacent acceleration correlation function is developed to improve robustness of reference point-defined method. The performance of hybrid identification method is investigated numerically (8-DOF lumped mass model and cantilever beam) and experimentally (ASCE Benchmark structure). Furthermore, hybrid HJDEA and gradient search method on damage identification accuracy and efficiency are discussed. Following conclusions can be summarized from this study:

(1) The proposed hybrid algorithm can effectively combine the merits of strong local search ability of Jaya and global search ability of DE. In addition, HJDEA has the advantages of simple structure, easy operation and robust performance for the reason that any algorithm-specific parameters are not required.
(2) Compared with GA, PSO and Jaya algorithm, identification results demonstrate HJDEA is more accurate and efficient to identify structural stiffness and mass parameters under white noise excitation, owing to its ability to better achieve the balance between global exploration and local exploitation.
(3) Adjacent acceleration correlation function has competitive performance with reference point-defined methods, while it is more robust to obtain satisfactory identification results because of its reference point-free characteristic. The proposed identification method based on HJDEA and correlation function is able to accurately identify the damage location and extent even with 20% noise pollution.
(4) Hybrid HJDEA and gradient search method can initially implement coarse global search to the neighborhood of the optimal solution by HJDEA and then take it as initial value in the subsequent gradient search, which is a promising alternative to further improve damage identification accuracy and efficiency in a relatively small search space.
(5) The proposed hybrid identification method could successfully identify structural stiffness and mass damages with noise-polluted output-only responses under white noise excitation, while more complex and practical identification of structural stiffness, mass and damping parameters considering uncertainties, such as modelling error, temperature variation, boundary stiffness reduction etc. still need to be investigated in the future.

CRediT authorship contribution statement

Guangcai Zhang: Writing – original draft, Investigation, Software. **Chunfeng Wan:** Supervision, Conceptualization, Writing – review & editing. **Xiaobing Xiong:** Methodology, Visualization, Investigation. **Liyu Xie:** Writing – review & editing. **Mohammad Noori:** Visualization. **Songtao Xue:** Funding acquisition, Conceptualization, Writing – review & editing.

Declaration of Competing Interest

The authors declare that they have no known competing financial interests or personal relationships that could have appeared to influence the work reported in this paper.

Acknowledgments

The author(s) would like to thank the anonymous reviewers for their detailed and fruitful remarks. The author(s) disclosed receipt of the following financial support for the research, authorship, and/or publication of this article: This research was supported by the Key Program of Intergovernmental International Scientific and Technological Innovation Cooperation (2021YFE0112200), the Japan Society for Promotion of Science (Kakenhi No. 18K04438), and the Tohoku Institute of Technology research Grant.

References

[1] W. Fan, P.Z. Qiao, Vibration-based damage identification methods: a review and comparative study, Struct. Health Monit. 10 (1) (2011) 83–111.
[2] O.S. Salawu, Detection of structural damage through changes in frequency: a review, Eng. Struct. 19 (9) (1997) 718–723.
[3] R. Gorgin, Damage identification technique based on mode shape analysis of beam structures, Structures 27 (2020) 2300–2308.
[4] V. Srinivas, K. Ramanjaneyulu, C.A. Jeyasehar, Multi-stage approach for structural damage identification using modal strain energy and evolutionary optimization techniques, Struct. Health Monit. 10 (2) (2011) 219–230.
[5] R. Janeliukstis, S. Rucevskis, M. Wesolowski, et al., Experimental structural damage localization in beam structure using spatial continuous wavelet transform and mode shape curvature methods, Measurement 102 (2017) 253–270.
[6] J.N. Yang, S.W. Pan, S. Lin, Least-squares estimation with unknown excitations for damage identification of structures, J. Eng. Mech. 133 (1) (2007) 12–21.
[7] S. Sen, B. Bhattacharya, Online structural damage identification technique using constrained dual extended Kalman filter, Struct. Control Health Monit. 24 (9) (2017), e1961.
[8] E.N. Chatzi, A.W. Smyth, Particle filter scheme with mutation for the estimation of time-invariant parameters in structural health monitoring applications, Struct. Control Health Monit. 20 (7) (2013) 1081–1095.
[9] Z.R. Lu, J. Zhou, L. Wang, On choice and effect of weight matrix for response sensitivity-based damage identification with measurement and model errors, Mech. Syst. Signal Pr 114 (2019) 1–24.
[10] A. Katunin, Vibration-based spatial damage identification in honeycomb-core sandwich composite structures using wavelet analysis, Compos. Struct. 118 (2014) 385–391.
[11] Z.C. Yang, Z.F. Yu, H. Sun, On the cross correlation function amplitude vector and its application to structural damage detection, Mech. Syst. Signal Pr 21 (7) (2007) 2918–2932.
[12] Y. Hui, S.S. Law, C.J. Ku, Structural damage detection based on covariance of covariance matrix with general white noise excitation, J. Sound Vib. 389 (2017) 168–182.

[13] P.H. Ni, Xia Yong, S.S. Law, et al., Structural damage detection using auto/cross-correlation functions under multiple unknown excitations, Int. J. Struct. Stab. Dyn. 14 (5) (2014), 1440006.
[14] X.J. Wang, G.C. Zhang, X.M. Wang, et al., Output-only structural parameter identification with evolutionary algorithms and correlation functions, Smart Mater. Struct. 29 (3) (2020), 035018.
[15] M.Y. Zhang, Z.C. Yang, L. Wang, et al., Damage locating for composite beam structure by cross correlation analysis without reference node, Eng. Mech. 28 (11) (2011) 166–169.
[16] S.M.C.M. Randiligama, D.P. Thambiratnam, T.H.T. Chan, et al., Damage assessment in hyperbolic cooling towers using mode shape curvature and artificial neural networks, Eng. Fail. Anal. 129 (2021), 105728.
[17] W.S. Na, A portable bolt-loosening detection system with piezoelectric-based nondestructive method and artificial neural networks, Struct. Health Monit. 134 (2021) 12–34.
[18] Y. Azimi, S.H. Khoshrou, M. Osanloo, Prediction of blast induced ground vibration (BIGV) of quarry mining using hybrid genetic algorithm optimized artificial neural network, Measurement 147 (2019), 106874.
[19] P.A. Sankar, R. Machavaram, K. Shankar, System identification of a composite plate using hybrid response surface methodology and particle swarm optimization in time domain, Measurement 55 (2014) 499–511.
[20] H.S. Tang, S.T. Xue, C.X. Fan, Differential evolution strategy for structural system identification, Comput. Struct. 86 (21–22) (2008) 2004–2012.
[21] H.L. Chen, Z.H. Liu, B. Wu, et al., An intelligent algorithm based on evolutionary strategy and clustering algorithm for Lamb wave defect location, Struct. Health Monit. 20 (4) (2021) 2088–2109.
[22] F.A.C. Viana, G.I. Kotinda, D.A. Rade, et al., Tuning dynamic vibration absorbers by using ant colony optimization, Comput. Struct. 86 (13–14) (2008) 1539–1549.
[23] S. Feng, J.Q. Jia, Acceleration sensor placement technique for vibration test in structural health monitoring using microhabitat frog-leaping algorithm, Struct. Health Monit. 17 (2) (2018) 169–184.
[24] H. Sun, H. Luş, R. Betti, Identification of structural models using a modified Artificial Bee Colony algorithm, Comput. Struct. 116 (2013) 59–74.
[25] H.Y. Zhou, G.C. Zhang, X.J. Wang, et al., Structural identification using improved butterfly optimization algorithm with adaptive sampling test and search space reduction method, Structures 33 (2021) 2121–2139.
[26] P. Ghannadi, S.S. Kourehli, M. Noori, et al., Efficiency of grey wolf optimization algorithm for damage detection of skeletal structures via expanded mode shapes, Adv. Struct. Eng. 23 (13) (2020) 2850–2865.
[27] S. Das, P. Saha, Performance of swarm intelligence based chaotic meta-heuristic algorithms in civil structural health monitoring, Measurement 169 (2021), 108533.
[28] L.S. Tan, Z. Zainuddin, P. Ong, Wavelet neural networks based solutions for elliptic partial differential equations with improved butterfly optimization algorithm training, Appl. Soft Comput. 95 (2020), 106518.
[29] Z.H. Ding, J. Li, H. Hao, et al., Nonlinear hysteretic parameter identification using an improved tree-seed algorithm, Swarm Evol. Comput. 46 (2019) 69–83.
[30] J.G. Zheng, Y.L. Wang, A Hybrid Multi-Objective Bat Algorithm for Solving Cloud Computing Resource Scheduling Problems, Sustainability 13 (14) (2021) 7933.
[31] R.V. Rao, Jaya: An Advanced Optimization Algorithm and its Engineering Applications. Springer, Cham; 2018.
[32] R.V. Rao, Jaya: A simple and new optimization algorithm for solving constrained and unconstrained optimization problems, Int. J. Ind. Eng. Comp. 7 (1) (2016) 19–34.
[33] X.Z. Jian, Z.Y. Weng, A logistic chaotic JAYA algorithm for parameters identification of photovoltaic cell and module models, Optik 203 (2020), 164041.
[34] R.V. Rao, A. Saroj, Constrained economic optimization of shell-and-tube heat exchangers using elitist-Jaya algorithm, Energy 128 (2017) 785–800.
[35] B.M. Alshammari, A. Farah, K. Alqunun, et al., Robust design of dual-input power system stabilizer using chaotic JAYA algorithm, Energies 14 (17) (2021) 5294.
[36] L.J. He, W.F. Li, R. Chiong, et al., Optimising the job-shop scheduling problem using a multi-objective Jaya algorithm, Appl. Soft Comput. 111 (2021), 107654.
[37] K. Thirumoorthy, K. Muneeswaran, A hybrid approach for text document clustering using Jaya optimization algorithm, Expert Syst. Appl. 178 (2021), 115040.
[38] K.J. Yu, J.J. Liang, B.Y. Qu, et al., Parameters identification of photovoltaic models using an improved JAYA optimization algorithm, Energy Convers. Manage. 150 (2017) 742–753.
[39] K.J. Yu, B.Y. Qu, C.T. Yue, et al., A performance-guided JAYA algorithm for parameters identification of photovoltaic cell and module, Appl. Energy 237 (2019) 241–257.
[40] A. Farah, A. Belazi, A novel chaotic Jaya algorithm for unconstrained numerical optimization, Nonlinear Dyn. 93 (3) (2018) 1451–1480.
[41] W. Warid, H. Hizam, N. Mariun, et al., A novel quasi-oppositional modified Jaya algorithm for multi-objective optimal power flow solution, Appl. Soft Comput. 65 (2018) 360–373.
[42] Z.P. Chen, L. Yu, A new structural damage detection strategy of hybrid PSO with Monte Carlo simulations and experimental verifications, Measurement 122 (2018) 658–669.
[43] H.Y. Zhou, G.C. Zhang, X.J. Wang, et al., A hybrid identification method on butterfly optimization and differential evolution algorithm, Smart Struct. Syst. 26 (3) (2020) 345–360.
[44] S. Shirgir, B.F. Azar, A. Hadidi, Reliability-based simplification of Bouc-Wen model and parameter identification using a new hybrid algorithm, Structures 27 (2020) 297–308.
[45] Y. Liang, S. Hu, W. Guo, et al., Abrasive tool wear prediction based on an improved hybrid difference grey wolf algorithm for optimizing SVM, Measurement 187 (2022), 110247.
[46] Z.H. Ding, Y.L. Zhao, Z.R. Lu, Simultaneous identification of structural stiffness and mass parameters based on Bare-bones Gaussian Tree Seeds Algorithm using time-domain data, Appl. Soft Comput. 83 (2019), 105602.
[47] R.A. Ibrahim, E.M. Abd, S.F. Lu, Chaotic opposition-based grey-wolf optimization algorithm based on differential evolution and disruption operator for global optimization, Expert Syst. Appl. 108 (2018) 1–27.
[48] Y.C. Li, M.X. Han, Q.L. Guo, Modified whale optimization algorithm based on tent chaotic mapping and its application in structural optimization, KSCE J. Civ. Eng. 24 (12) (2020) 3703–3713.
[49] Z. Zhang, C.G. Koh, W.H. Duan, Uniformly sampled genetic algorithm with gradient search for structural identification–Part I: Global search, Comput. Struct. 88 (15–16) (2010) 949–962.
[50] Y.H. Shi, R.C. Eberhart, Empirical study of particle swarm optimization, in: Proceeding of the IEEE Congress on Evolutionary Computation, Washington, DC, USA, 6-9 July 1999, pp. 1945–1950. New York: IEEE.
[51] E.A. Johnson, H.F. Lam, L.S. Katafygiotis, et al., Phase I IASC-ASCE structural health monitoring benchmark problem using simulated data, J. Eng. Mech. 130 (1) (2004) 3–15.
[52] H. Sun, R. Betti, A hybrid optimization algorithm with Bayesian inference for probabilistic model updating, Comput.-Aided Civ. Infrastruct. Eng. 30 (8) (2015) 602–619.